JOURNAL OF VIROLOGY, Dec. 1996, p. 8590–8605 Vol. 70, No. 12
0022-538X/96/$04.00+0

Synergistic Interactions between Overlapping Binding Sites for the Serum Response Factor and ELK-1 Proteins Mediate both Basal Enhancement and Phorbol Ester Responsiveness of Primate Cytomegalovirus Major Immediate-Early Promoters in Monocyte and T-Lymphocyte Cell Types

YU-JIUN CHAN,[1] CHUANG-JIUN CHIOU,[2] QI HUANG,[1] AND GARY S. HAYWARD[1,2]*

The Molecular Virology Laboratories, Departments of Pharmacology and Molecular Sciences[1] and Oncology,[2] Johns Hopkins University School of Medicine, Baltimore, Maryland 21205

Received 20 May 1996/Accepted 21 August 1996

Cytomegalovirus (CMV) infection is nonpermissive or persistent in many lymphoid and myeloid cell types but can be activated in differentiated macrophages. We have shown elsewhere that both the major immediate-early gene (MIE) and lytic cycle infectious progeny virus expression can be induced in otherwise nonpermissive monocyte-like U-937 cell cultures infected with either human CMV (HCMV) or simian CMV (SCMV) by treatment with the phorbol ester 12-*O*-tetradecanoylphorbol-13-acetate (TPA). Two multicopy basal enhancer motifs within the SCMV MIE enhancer, namely, 11 copies of the 16-bp cyclic AMP response element (CRE) and 3 copies of novel 17-bp serum response factor (SRF) binding sites referred to as the SNE (SRF/NFκB-like element), as well as four classical NFκB sites within the HCMV version, contribute to TPA responsiveness in transient assays in monocyte and T-cell types. The SCMV SNE sites contain potential overlapping core recognition binding motifs for SRF, Rel/NFκB, ETS, and YY1 class transcription factors but fail to respond to either serum or tumor necrosis factor alpha. Therefore, to evaluate the mechanism of TPA responsiveness of the SNE motifs and of a related 16-bp SEE (SRF/ETS element) motif found in the HCMV and chimpanzee CMV MIE enhancers, we have examined the functional responses and protein binding properties of multimerized wild-type and mutant elements added upstream to the SCMV MIE or simian virus 40 minimal promoter regions in the U-937, K-562, HL-60, THP-1, and Jurkat cell lines. Unlike classical NFκB sites, neither the SNE nor the SEE motif responded to phosphatase inhibition by okadaic acid. However, the TPA responsiveness of both CMV elements proved to involve synergistic interactions between the core SRF binding site (CCATATATGG) and the adjacent inverted ETS binding motifs (TTCC), which correlated directly with formation of a bound tripartite complex containing both the cellular SRF and ELK-1 proteins. This protein complex was more abundant in U-937, K-562, and HeLa cell extracts than in Raji, HF, BALB/c 3T3, or HL-60 cells, but the binding activity was altered only twofold after TPA treatment. A 40-fold stimulation of chloramphenicol acetyltransferase activity mediated by four tandem repeats of the SNE could be induced within 2 h (and up to 250-fold within 6 h) after addition of TPA in DNA-transfected U-937 cells, indicating that the stimulation appeared likely to be a true protein kinase C-mediated signal transduction event rather than a differentiation response. Slight differences in the sequence of the core SRF binding site compared with that of the classical c-Fos promoter serum response element, together with differences in the spacing between the SRF and ETS motifs, appear to account for the inability of the SCMV SNEs to respond to serum induction.

The mechanisms controlling immediate-early (IE) gene regulation in cytomegalovirus (CMV) are of crucial importance for understanding cell type specificity, progression of the lytic cycle cascade, and the outcome of host-virus interactions, as well as for defining how the virus reactivates from a persistent or latent state, which is believed to occur predominantly in monocytes, myeloid stem cells, and perhaps T cells (20, 31, 39, 61, 64, 78, 79, 86). The major IE (MIE) gene products, which are autoregulatory transactivators that trigger the expression of downstream viral genes in transient assays, are expected to be key players governing the productive cycle and are often found to be repressed in nonpermissive or latent infections (40, 41, 50, 54, 65, 71). Therefore, to explore the mechanism of CMV reactivation, it is important to determine how the virus detects and responds to changes in the differentiation or activation state of host cells that have the potential to control viral MIE gene expression. Although in primary infections, the choice between lytic or inapparent infection is probably influenced by incoming virion factors (49) as well as by preexisting cellular transcription factors, reactivation from the latent state must be mediated first by inducible host cell factors acting at the transcriptional level on the MIE enhancer. Several studies have shown that agents that alter either the differentiation or activated states of monocyte or myeloid lineage cells in culture can alter the degree of permissivity to CMV (17, 18, 73, 79, 86). Furthermore, we have recently demonstrated that the addition of the phorbol ester 12-*O*-tetradecanoylphorbol-13-acetate (TPA) to otherwise completely nonpermissive U-937 cells, even at up to 12 days after infection by either human CMV (HCMV) or simian CMV (SCMV), can lead both to increased MIE mRNA and protein expression and to induction of low

* Corresponding author. Mailing address: Department of Pharmacology and Molecular Sciences, Johns Hopkins University School of Medicine, 725 N. Wolfe St., WBSB 317, Baltimore, MD 21205. Phone: (410) 955-8684. Fax: (410) 955-8685. Electronic mail address: Gary.Hayward@qmail.bs.jhu.edu.

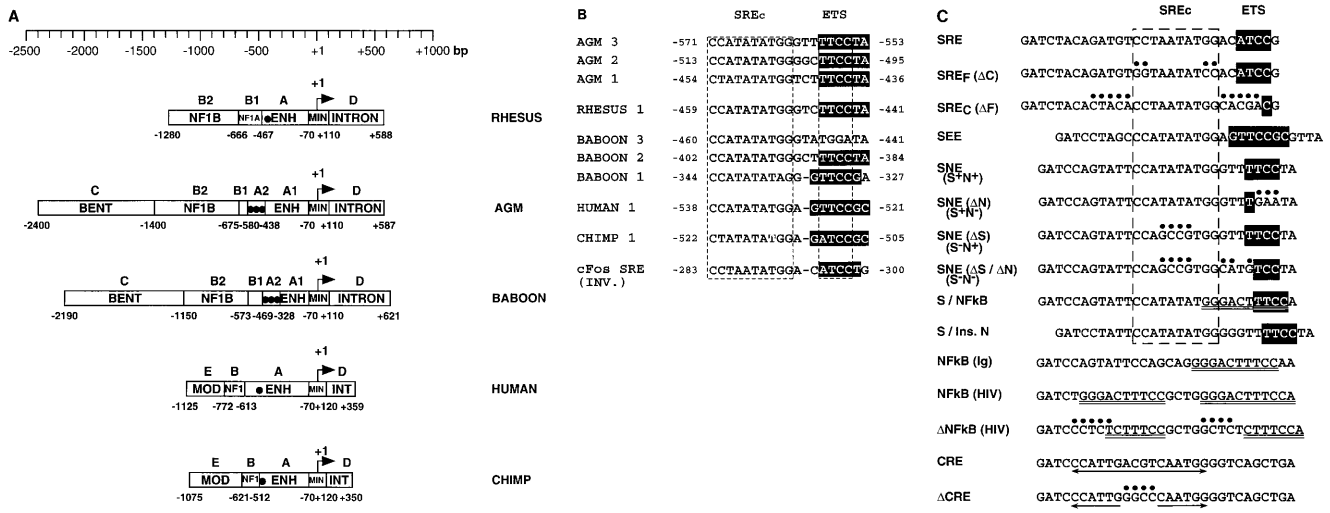

FIG. 1. (A) Organization of the MIE gene control regions in five Old World primate CMVs. The diagram represents a simplified summary of data compiled by Alcendor et al. (1). Position +1 represents the start site for all IE class transcripts encoding both IE1 and IE2 proteins. Each control region is considered to have a minimal promoter and leader region (MIN) between positions −70 to +110 encompassing several ATF and SP-1 sites, the TATATAA box, and the highly conserved first noncoding exon, as well as the fully conserved *cis* repression sequence (CRS) at the cap site, which represents a binding site for the viral IE2 protein and correlates with negative autoregulation. Regulatory domain ENH-A1 contains multicopy CRE, NFκB, AP-1, and series II and IV motifs and behaves as a high basal plus cAMP- and TPA-inducible enhancer. Domain ENH-A2 contains multiple SRF binding sites, including the SNE and SEE motifs examined in this study (solid circles). Domain B represents a cluster of overlapping palindromic high-affinity NF-1 and YY1 binding sites that includes up to 23 copies of 30-bp tandem repeats in all three circopithecoid SCMV species (NF1-B), and 16- to 21-bp tandem repeats in the NF1-A region of rhesus SCMV, but only three to four sites in HCMV and chimpanzee SCMV. Domain C represents a large intrinsically bent DNA domain in AGM and baboon SCMV but is absent in the others. Domain D includes clustered NF1 and series VII repeats plus isolated YY1, SP-1, SRE, and other motifs within the large first intron regions. Domain E denotes the negatively acting MOD domain encompassing several YY1 sites and a cluster of approximately 20 CGATA interspersed repeats in both HCMV and chimpanzee SCMV. (B) DNA sequences of all nine known series V and III SNE or SEE motifs from within the primate CMV MIE enhancer regions. These are aligned with the inverted (INV.) orientation of the SRE from the c-Fos promoter. The core 10-bp SRF binding sites (SRF_c) are boxed. Note that eight of the nine SCMV motifs have the sequence CCATATATGG, which differs from the classical CCTAATATGG sequence for the c-Fos version, which for proper alignment is shown inverted from its natural polarity in the c-Fos promoter. The adjacent ETS class inverted core GGAA motifs on the right are also boxed, with the two types of characteristic consensus motifs of the SNE (TAGGAA) and SEE (GCGGAAC) subtypes highlighted. The core ETS motif (GGAT) in the SRE is also highlighted and italicized. Note that only the three SEE sites (human, chimpanzee, and baboon site 1) show the same N2 spacing as does the SRE core ETS motif, whereas the others are all N3. The highlighted SEE motif is also a close match to the specific recognition motif GCGGAAC for the ETS class protein GABP (43). Baboon site 3 is tentatively included as an SNE because it contains a potential core ETS motif GGAT, although in inverted orientation relative to the others. (C) Oligonucleotide probes used in this study. Only the sequences of the top strands of each annealed pair are shown. The core SRF binding sites are boxed, and the core inverted ETS motifs including the consensus GABP site in the HCMV SEE are highlighted. Altered base pairs are indicated by solid overhead circles, and the double underline denotes the classical Ig kappa NFκB motif GGGACTTTCC or the 16-bp palindrome series I CRE motif CCATTGACGTCAATGG. The spacing mutant S/InsN contains two added guanines between the core SRF and ETS motifs. In each case, annealing with the complementary strand creates 4-bp *Bam*HI and *Bgl*II 5′ overhangs for cloning purposes that are filled in with T4 polymerase during end labeling for use as EMSA probes.

levels of infectious progeny virions as assayed by cocultivation with HF cells (11).

The CMV MIE gene products, the IE1 and IE2 proteins, are presumed to be involved directly in regulating subsequent gene expression during the viral lytic cascade, as well as acting as potential triggers of the switch between latent and lytic infection (25, 34, 35, 59, 85). The CMV IE1 acidic phosphoprotein is translated from a 1.95-kb mRNA, which contains exons 1 to 4 from the MIE gene and is a 68- to 72-kDa (HCMV) or 94-kDa (SCMV) phosphorylated nuclear protein (34, 42, 75). However, the exact function of the IE1 protein is not clear. The intact IE2 phosphorylated nuclear protein is translated from a 2.25-kb mRNA containing exons 1, 2, 3, and 5 that is generated from the MIE gene by alternative splicing. IE2 functions both as a powerful nonspecific transactivator and as a specific repressor that negatively autoregulates the MIE promoter (25, 59, 74). The dimeric 80-kDa form of the IE2 protein in particular appears to play an important role in both up-regulating early gene products and down-regulating its own gene expression through specific binding to the palindromic *cis* repression sequence, CGTTTN4AACCG, located at the cap site of both the HCMV and SCMV MIE regions (12, 45, 57, 58).

The entire MIE enhancer/promoter region has been sequenced for human, chimpanzee, African green monkey (AGM), baboon, and rhesus CMVs (1, 2, 6, 10, 36, 82) as well as for mouse and rat CMVs. The genomic structures of the five primate CMV MIE enhancer regions, which range in size from 1,500 to 3,000 bp, show two distinct patterns of subregion organization exemplified by the great ape CMV versions (human and chimpanzee) and the three circopithecoid versions (Fig. 1A). In HCMV, the whole MIE_H regulatory region (previously referred to as IE68), which spans from −1125 upstream to +360 downstream from the transcription start point, can be considered as five subregions with different functional roles. These are referred to as the far-upstream modulatory region (MOD), the nuclear factor 1 binding site region (NF1), the proximal enhancer region (ENH), the minimal promoter plus leader region (MIN), and the downstream intron control region (INT). The HCMV proximal ENH region between positions −613 and −70 contains four sets of interspersed multicopy transcription factor binding sites (referred to as 19-, 16-, 18-, and 21-bp elements) and represents the principal *cis*-acting basal enhancer region (1, 22, 82). In addition, two retinoic acid (RA) response elements have been identified within the ENH region and shown to mediate induction in human teratocarcinoma (NTera2) cells after RA stimulation (21). The SCMV(AGM) enhancer/promoter (previously referred to as

IE94) includes a proximal ENH region mapping between −570 to −69, which also consists of several sets of interspersed repeated sequences (series I to V) that closely resemble those in HCMV, except that they differ greatly in both copy number and organization (9, 34, 36).

The HCMV MOD region contains several consensus NF-1 and YY1 binding sites and has been proposed to play a negative regulatory role in teratocarcinoma cell lines (54). In contrast, the circopithecoid SCMV upstream regions have substituted additional larger domains in place of the HCMV MOD region. In AGM, rhesus, and baboon SCMVs, the first extended subregion (NF1-B) contains approximately 20 copies of 30-bp tandemly repeated high-affinity palindromic NF-1 binding sites [(T)TGG(C/A)N_5GCCAA] (1, 2, 36) with overlapping and interspersed high-affinity YY1 binding sites (CGCCATT TT). In AGM and baboon SCMV, a second further upstream subregion (BENT in Fig. 1A) ending at positions −2400 and −2160, respectively, contains a 1,000-bp long A+T-rich bent DNA domain (1, 10). The NF1 cluster and bent DNA region in the far-upstream SCMV MIE_S control region do not have basal enhancer or modulatory properties in transient assays but have been suggested to play an indirect role in the constitutive SCMV MIE_S expression in human NTera2 teratocarcinoma cells, even in the absence of RA stimulation (10, 36, 40). In contrast, the HCMV MOD region contains many fewer NF1 sites and HCMV MIE_H gene expression occurs only after RA stimulation in NTera2 cells (23, 40, 41).

Among the repetitive ENH motifs in primate CMV MIE regions, the cyclic AMP (cAMP) response element (CRE) sites (series I or 19-bp elements) and the NFκB sites (series III or 18-bp elements) have received the most attention. Both have been shown convincingly to be functionally relevant components of basal and induced enhancer activity when added to heterologous minimal promoters, as well as to mediate protein kinase A (PKA) or PKC signal transduction pathways that activate MIE gene expression. Additive effects of between 5 and 11 of the 16-bp palindromic series I repeats CCATTGA CGTCAATGG, which encompass 8-bp core consensus CREB binding sites, proved to be responsible for both basal enhancement and cAMP-induced activities in the K-562 erythroleukemia cell line, as well as the responses to cAMP and phytohemagglutinin-plus-phorbol myristate acetate treatment in Jurkat T cells in transient transfection assays using sets of deleted MIE enhancer-driven reporter genes or multicopy consensus CRE oligonucleotides linked to heterologous minimal promoters (9, 31, 72). Four or five 18-bp repeats with the core consensus GGGGACTTTCC, which closely resemble the classical immunoglobulin (Ig) kappa light-chain NFκB site, occur in both the human and chimpanzee CMV MIE enhancers and were postulated to be *cis*-acting phorbol myristate acetate-responsive regulatory elements in Jurkat cells (64). In contrast, the SCMV MIE_S contains several variant nonconsensus NFκB-related elements (series IIIB); however, these proved to bind preferentially to KBF1 or other Rel proteins (p50:p50) present in Raji B-cell extracts but only weakly to NFκB itself (p65:p50) (13a). Several consensus AP-1 sites in the HCMV MIE_H enhancer could also potentially mediate TPA responses, but the SCMV MIE_S enhancer region contains no compelling classical consensus motifs for either NFκB or AP-1.

We have shown elsewhere that the SCMV MIE_S series I CREs also respond directly to TPA in transient assays in monocyte and T-cell types (11), but another candidate transcription factor for mediating the TPA-induced signal transduction pathway in SCMV has turned out to be the serum response factor (SRF), which is the subject of this study. Three copies of an SRF core consensus binding site motif referred to previously as the series V repeats (10) each overlap with a series IIIB motif, producing novel elements referred to as SNE (SRF/NFκB-like elements) with the consensus sequence CCA TATATGGGTTTTCC. These all occur within the SCMV MIE ENH-A2 subregion between positions −573 and −444, which displays basal enhancer characteristics in U-937 cells but fails to respond to serum induction in NIH 3T3 cells (10). In other studies, we found that whereas the ENH-A1 and ENH-A2 domains each respond independently to a level of between 8- and 15-fold to TPA induction in immature U-937 cells, neither does so alone in the more mature THP-1 cells (11). However, the combination of ENH-A1 and ENH-A2 domains restores the ability to respond 5.5-fold to TPA in THP-1 cells. Furthermore, reconstruction experiments indicated that two tandem copies of a 30-mer SNE oligonucleotide added upstream to a minimal SCMV MIE_m(−69/+30) promoter reporter gene were required to obtain significant (i.e., 15- to 20-fold) TPA responses in U-937 cells, whereas four copies were required in HL-60 cells (11). The present studies were designed to explore the mechanism of TPA induction associated with the SNE motifs.

Serum response elements (SREs) have been found in several cellular IE gene promoters, including c-*fos* and *egr-1* promoters. They are usually regulated by extracellular signals including serum, growth factors, mitogens, and phorbol esters (83). Many studies on the mechanism of c-Fos SRE responsiveness have found that SRF and a ternary complex factor (TCF), which cannot bind to the SRE motif by itself (69), form a cooperative DNA-bound complex. The SRF protein recognizes the core c-Fos SRF site (CCATATTAGG) and the TCF protein contacts both the SRF protein and an adjacent ETS binding motif (CAGGAT) that lies 2 bp 5′ to the core SRF motif (15, 30, 69, 70). Here we report that SRF-related SNEs are consistently found in several different primate MIE ENH-A2 regions and demonstrate that the HCMV MIE_H region also contains a single SRF-related functional element at −538 to −523, which we refer to as an SEE (SRF/ETS element) because of the presence of both SRF and potential consensus ETS class GA-binding protein (GABP) binding sites (43), as well as the absence of NFκB-related motifs. Although differing in the spacing between the SRF and ETS motifs, both the HCMV SEE and SCMV SNE motifs were found to bind in vitro to the cellular SRF and to form a ternary complex with an ETS family protein. They both also responded rapidly to TPA induction in monocyte and lymphoid cell lines, but unlike NFκB sites, they failed to be induced by okadaic acid (OA) treatment to inhibit phosphatases. In the SCMV SNEs, mutational analysis revealed that both the overlapping SRF and ETS motifs are essential for activity and that they have synergistic effects on both basal enhancement and TPA responsiveness, suggesting that a viral version of this cellular protein-protein interaction is involved in regulating the CMV MIE transcriptional enhancer.

MATERIALS AND METHODS

Cells and reagents. Suspension cell lines (human K-562 [erythroleukemia], human U-937 [immature monocyte-like histiocytic lymphoma], human HL-60 [promyelocytic leukemia], human Jurkat [T-cell leukemia], and human THP-1 [mature monocytic leukemia]) were grown in RPMI 1640 medium plus 10% fetal calf serum in a 37°C incubator supplied with 5% CO_2. Adherent cells such as human HF, mouse BALB/c 3T3, and monkey Vero cells were grown in Dulbecco modified Eagle medium plus 10% fetal calf serum. K-562, U-937, HL-60, and Jurkat cells were obtained from the American Type Culture Collection (Rockville, Md.). THP-1 cells were kindly provided by James Hildreth (Johns Hopkins School of Medicine). TPA (Sigma) was dissolved in dimethyl sulfoxide to a concentration of 20 μg/ml as a stock solution and used at a working concentration of 50 ng/ml for each TPA stimulation experiment. OA was purchased from

Boehringer Mannheim Co. and dissolved in ethanol as a 100× stock solution. Rabbit polyclonal antibodies recognizing ELK-1 (sc-355), ETS-1/2 (sc-112), ETS-1 (sc-111), and PEA3 (sc-113) were purchased from Santa Cruz Biotechnology, Inc. PU1 antibody was kindly provided by Richard A. Maki. GABPα (C95) and GABPβ (C96) rabbit anti-mouse antibodies were gifts from Fabienne de la Brousse (Tularik Inc., San Francisco, Calif.). HeLa-S3 and U-937 nuclear pellets were purchased from the Cell Culture Center (Cellex Biosciences Inc., Minneapolis, Minn.).

Construction of target reporter genes. The three different minimal reporter gene backgrounds used, the SCMV(AGM) $MIE_m(-69/+30)$-chloramphenicol acetyltransferase (CAT) gene in pCJC81, the simian virus 40 (SV40) A10(−150/+58)-CAT gene in pA10-CAT, and the HCMV $IES_m(-55/+80)$-CAT gene in pYJC90, have been described previously (8, 10). The human immunodeficiency virus type 1 (HIV-1) long terminal repeat (LTR) targets containing the wild-type NFκB sites in LTR(−483/+80)-CAT and a version with triple-point mutations in both copies of the NFκB sites LTR(ΔNFκB)-CAT are carried in plasmids pUR-III and mpUR-III (53). A single-copy 23-bp oligonucleotide form of the c-Fos SRE placed in the herpes simplex virus (HSV) thymidine kinase-CAT promoter background was obtained from Barbara Christie and Dan Nathans (13).

Inserted 30-bp oligonucleotides representing two tandem 30-bp copies of the wild-type or mutant SCMV consensus series I CRE motif as $(CRE)_2$/A10-CAT in pYNC55 and $(\Delta CRE)_2$/A10-CAT in pYNC70, or as two or four copies of the same wild-type CRE motif in the SCMV minimal MIE_S background as $(CRE)_2$/MIE_m-CAT in pYNC45 and $(CRE)_4$/MIE_m-CAT in pYNC50, were all described previously by Chang et al. (9). Similar constructions containing two or four tandem 30-bp copies of the wild-type SCMV SRF/NFκB-like motifs (LGH218/219) as $(SNE)_2$/MIE_m-CAT in pCJC112, $(SNE)_4$/MIE_m-CAT in pCJC114, $(SNE)_2$/A10-CAT in pCJC12, and $(SNE)_4$/A10-CAT in pCJC14 were prepared. Mutant versions of the SCMV SNEs included a point mutant in the SRF submotif (LGH399/400) as $(S^-N^+)_2$/MIE_m-CAT in pCJC132 and $(S^-N^+)_2$/A10-CAT in pCJC32, a point mutant in the ETS/NFκB-like submotif (LGH324/325) as $(S^+N^-)_2$/MIE_m-CAT in pCJC152 and $(S^+N^-)_2$/A10-CAT in pCJC52, and a double-point mutant in both submotifs (LGH322/323) as $(S^-N^-)_2$/MIE_m-CAT in pCJC172 and $(S^-N^-)_2$/A10-CAT in pCJC72.

The $(SEE)_4$/MIE_m-CAT gene (pYJC294B), $(NF\kappa B)_4$/MIE_m-CAT gene (pYJC304B), $(SkB)_4$/MIE_m-CAT gene (pYJC224B), and $(S/InsN)_4$/MIE_m-CAT gene (pYJC244B) each contain four tandemly repeated copies of the synthetic 30-bp oligonucleotides for the wild-type HCMV overlapping SRF/ETS site (LGH814/815), the wild-type classical Ig kappa NFκB site (LGH816/817), an SCMV SRF plus modified classical NFκB site (LGH801/802), and two extra inserted G's between the SCMV SRF and NFκB-like site (LGH803/804), respectively, placed in the backward orientation at the 5′ *Bgl*II site in the SCMV minimal $MIE_m(-69/+30)$-CAT gene background of pCJC81. The $(SRE)_2$/MIE_m-CAT gene (pYJC262A) and the $(SRE_c)_2$/MIE_m-CAT gene (pYJC282A) each contained two copies of the synthetic 30-bp oligonucleotides containing either the wild-type c-Fos SRE site (SRF plus ELK) (LGH638/639) or core SRE site only (LGH642/643) placed in the forward orientation at the 5′ *Bgl*II site in the minimal SCMV MIE_m (−69/+30)-CAT gene background of pCJC81. The $(SEE)_4$/IES_m-CAT (pYJC384B), $(SRE)_4$/IES_m-CAT (pYJC414B), $(NF\kappa B)_4$/IES-CAT (pYJC784B), or $(SNE)_4$/IES-CAT (pYJC794B) gene contains four copies of the synthetic 30-bp oligonucleotides encompassing wild-type HCMV SEE (LGH814/815), wild-type c-Fos SRE (LGH638/639), wild-type Ig kappa NFκB (LGH816/817), or wild-type SCMV SNE (LGH218/219), respectively, placed in the backward orientation at the 5′ *Bam*HI site in the minimal HCMV $IES_m(-55/+80)$-CAT gene of pYJC90.

Transient DNA transfection and CAT assays. For U-937 or K-562 suspension cultures, the cells were grown to a cell density of 10^6/ml and cell viability was checked by the trypan blue exclusion method. Cells were transfected by the DEAE-dextran procedure used previously for B lymphocytes (47). Briefly, 2 to 4 μg of CsCl-prepared plasmid DNA was added to 5×10^6 cells in CaTBS transfection solution (0.5 mM $MgCl_2 \cdot 6H_2O$, 1 mM $CaCl_2$, 137 mM NaCl, 5 mM KCl, 0.3 mM $Na_2HPO_4 \cdot 12H_2O$, 25 mM Tris-HCl [pH 7.5]) containing 430 μg of DEAE-dextran per ml in a final volume of 350 μl at 37°C for 45 min. Cells were pelleted at 1,500 rpm for 10 min at 4°C and washed with 500 μl of serum-free RPMI medium. The transfected cells were grown in a 37°C in 5% CO_2 overnight and treated with TPA or OA 24 h later if needed. TPA was left in the medium at the final concentration of 50 ng/ml, or OA was left for 18 h at the concentrations described, and the cells were harvested for CAT assays.

CAT assays were carried out as described previously (59). Cells were pelleted in a microcentrifuge for 1 min at 12,000 rpm, washed with 1 ml of harvest buffer (40 mM Tris-HCl [pH 8.0], 150 mM NaCl, 1 mM EDTA), repelleted, frozen and thawed three times in 100 μl of 250 mM Tris-HCl (pH 7.9), and pelleted at 4°C for 10 min at 12,000 rpm. Seventy-five microliters of the supernatant was used for each reaction. Assays were carried out in 150 μl of a mixture containing 590 mM Tris-HCl (pH 7.9), 533 μM acetyl coenzyme A, and 0.1 μCi of [^{14}C]chloramphenicol at 37°C for 1 h. Chloramphenicol was extracted from the aqueous phase with 1 ml of ethyl acetate by vigorous vortex centrifugation at 12,000 rpm for 3 min at 20°C followed by drying in a vacuum centrifuge and resuspension in 20 μl of ethyl acetate. Acetylated and nonacetylated forms of chloramphenicol were separated by thin-layer polyethyleneimine-cellulose chromatography on glass plates (20 cm by 20 cm by 0.5 mm) (Curtin Matheson Scientific, Inc.), using chloroform-methanol at 19:1 as a solvent for 1 h. The radioactive spots were visualized by autoradiography and scraped off the thin-layer chromatography plates for measurement in a scintillation counter.

Nuclear extracts and electrophoretic mobility shift assays (EMSAs). Nuclear extracts were prepared by a modification of the method of Dignam et al. (16). Briefly, suspension cells were collected at a density of 10^6/ml and adherent cells were harvested with rubber scrapers. The cells were washed with PBS-A. Two packed cell volumes of buffer A containing 10 mM *N*-2-hydroxyethylpiperazine-*N*′-2-ethanesulfonic acid (HEPES; pH 7.9), 1.5 mM $MgCl_2$, 10 mM KCl, 0.5 mM dithiothreitol, and protease inhibitor mixture (0.1 mM TPCK, 1 mM TLCK, 0.5 mM phenylmethylsulfonyl fluoride, 1 μg of aprotinin per ml, 1 μg of leupeptin per ml, and 1 μg of pepstatin A per ml) were added to swell the cells on ice for 10 min. A Dounce homogenizer size B (7 ml) was used to rupture the cell membranes. The nuclei were collected at 3,000 rpm at 4°C and resuspended in high-salt buffer C (20 mM HEPES [pH 7.9], 25% [vol/vol] glycerol, 0.42 M NaCl, 1.5 mM $MgCl_2$, 0.2 mM EDTA, 0.5 mM dithiothreitol, protease inhibitor mixture) to extract nuclear proteins by rocking at 4°C for 1 h and removing the nuclear debris. The supernatant which contains nuclear proteins was aliquoted and stored at −70°C for later use.

DNA-protein binding reactions were set up in a final volume of 20 μl containing 10 mM HEPES (pH 7.5), 50 mM KCl, 1 mM EDTA buffer, 0.1% Triton-X 100, 5% glycerol, 0.1 mM dithiothreitol, and 0.1 mM phenylmethylsulfonyl fluoride, 5 to 10 μg of nuclear extracts, 1 μg of poly(dI-dC), and 5 fmol of the ^{32}P-end-labeled oligonucleotide DNA probe and incubated for 15 min at 20°C (48, 62). The DNA-protein complexes were resolved by EMSA through 4% polyacrylamide gels (acrylamide/bisacrylamide ratio of 29:1), using 0.5× Tris-borate-EDTA or 1× HEE buffer (10 mM HEPES [pH 7.3] adjusted with NaOH, 1 mM EDTA, and 0.5 mM EGTA) as the running buffer. Electrophoresis was carried out at 150 to 200 V for 60 to 120 min at 20°C, and the gels (18 by 20 cm) were dried for autoradiography. For antibody supershift experiments, antibodies (0.1 μg/μl, 1 μl) were added into the solutions after protein-DNA incubation for 30 min at 20°C, and the DNA-protein complexes were resolved in either 1% agarose or 4% polyacrylamide gels, using 0.5× Tris-borate-EDTA as the running buffer.

Labeling of synthetic oligonucleotides. Single-stranded oligonucleotides were synthesized by Scott Morrow (Johns Hopkins University School of Hygiene and Public Health) and purified by high-pressure liquid chromatography procedures. The two complementary strands (10 μg) of each oligonucleotide pair were heated to 65°C for 5 min in 100 μl of STE (100 mM NaCl, 10 mM Tris-HCl [pH 8.0], 1 mM EDTA) and annealed by slow cooling. The labeling reaction of 3′-recessed ends was carried out in 20 μl of solution containing 1 pmol of synthetic oligonucleotide (3 μl) per μl, 10× reaction buffer (2 μl), 10 mM dGTP-dCTP-dTTP mixture (1 μl), 3.3 pmol of [α-^{32}P]dATP (1 μl, 10 μCi) per μl, 1 U of the Klenow fragment of polynucleotide polymerase (1 μl) per μl, and 12 μl of H_2O at 20°C for 30 min. The labeled double-stranded oligonucleotides were separated from free nucleotides by centrifugation at 3,000 rpm for 5 min on Sephadex G-25 columns (Pharmacia catalog no. 17-0033-01).

RESULTS

Identification of novel conserved SRE-related motifs in all primate CMV MIE ENH-A2 regions. We have shown previously that the SCMV(AGM) MIE enhancer region contains two distinct subdomains, ENH-A1 (−414 to −69) and ENH-A2 (−604 to −485), that independently give high basal expression characteristics in Vero cells and that an important feature of the ENH-A2 domain is the presence of several potential consensus SRF binding motifs (referred to as series V elements) that indeed bind efficiently to SRF in in vitro EMSA experiments (10). To search for additional conserved elements of this type, we compared the ENH regions of each of five primate MIE regions, from human (6, 82), AGM (10, 36), rhesus (2), chimpanzee (1), and baboon (1) CMVs, and identified between one and three related motifs (Fig. 1A) that contain a core SRF consensus binding site (CCATATATGG) at the far-upstream end of the ENH region in each case. In addition, we noticed that their flanking regions often have similar sequences. In the SCMV(AGM) MIE regions, some of these resemble diverged NFκB-like binding sites (ATGGGG TTTCC) and include inverted generic core ETS class protein binding sites as well (GGAA or GGAT). The human and chimpanzee CMV versions in particular as well as baboon site 1 also not only match well to the specific consensus binding site for the ETS class GABP factor GCGGAAC (44) but also have different spacing (N2) compared with the others (N3) between

the SRF and ETS core motifs. Therefore, we refer to the SRF consensus sites and adjacent conserved sequences in the SCMV(AGM) MIE region as the SNE motifs (because of the overlapping SRF and NFκB-like binding elements) and to that of the equivalent sequence in the human and chimpanzee MIE region as well as to baboon site 1 as SEE motifs. Human, chimpanzee, and rhesus CMVs each contain only one such motif, whereas AGM and baboon CMVs both have three (Fig. 1B). The three SNE sites in the SCMV(AGM) MIE gene form part of a 3 × 58-bp imperfect tandem repeat region that overlaps the ENH-A2 region and are located between positions −579 and −561, −521 and −503, and −462 and −444 upstream relative to the mRNA transcriptional start site. The SEE site in the HCMV MIE enhancer lies between positions −538 and −522. The close resemblance between these CMV elements and the classical SRE motif from the c-*fos* promoter (present in inverted orientation relative to its TATAA box motif) is also illustrated in the alignments shown in Fig. 1C). Curiously, as we have shown elsewhere (10, 11), neither an ENH-A2 fragment (containing two tandemly repeated SNEs within their local natural promoter context) nor multimerized copies of the SNE motif gave serum responsiveness in NIH 3T3 or BALB/c 3T3 cells, although the latter responded strongly to TPA induction in U937 cells.

Synergism between the two overlapping subcomponents of the SNE motif. As suggested previously, the SNE or series V/IIIB motifs in the SCMV(AGM) enhancer appeared to be composed of two overlapping components, referred to here as the S and N submotifs, as judged from known binding to SRF and predicted matches to NFκB-like binding sites (10). To address the question of whether both submotifs in the SNE sequences are required for full function, we synthesized new 30-bp oligonucleotide versions that were mutated in either the S or N submotif or both (Fig. 1C), inserted them in place of the wild-type versions in the $(S^+N^+)_2$/MIE_m-CAT reporter gene to generate the $(S^-N^-)_2$/, $(S^+N^-)_2$/, and $(S^-N^+)_2$/MIE_m-CAT plasmids, and tested their activities in transient transfection assays after introduction into suspension culture cells by the DEAE-dextran procedure. Two copies of the wild-type SNE sites augmented basal activity 7.1-fold, and four copies increased the activity to 14-fold in immature monocyte-like U-937 cells (Fig. 2A). In addition, two copies of the wild-type SNE gave a more than 13-fold increase when TPA was added at 24 h after transfection, to yield a 94-fold total stimulation over basal levels obtained with the parent minimal MIE_m-CAT gene. In contrast, mutations in either the S component alone or both the S and N motifs totally abolished the basal enhancement and reduced the TPA responses to the levels obtained with the parent minimal promoter (3.5-fold), whereas mutations in the N site also severely diminished but did not obliterate either basal enhancement or TPA responses (3.7- and 3.8-fold, respectively, for the two-copy version [Fig. 2A]).

Transfer of synergistic TPA responsiveness to a heterologous minimal promoter. Because the TPA responses were so potent, the CAT enzyme levels obtained were often beyond the linear range with two or four copies of the wild-type SNE, especially in U-937 and K-562 cells when we used the SCMV MIE_m-CAT gene background. Therefore, we also tested another set of CAT reporter genes that contained the SV40 minimal promoter (pA10-CAT) with added upstream multimerized wild-type and mutant SNE motifs. The results again clearly demonstrated that in order to obtain both basal enhancement and TPA responses (which together totaled 30- and 130-fold increases for two and four copies of the wild-type SNE, respectively), both the S and N submotifs were required (Fig. 2B).

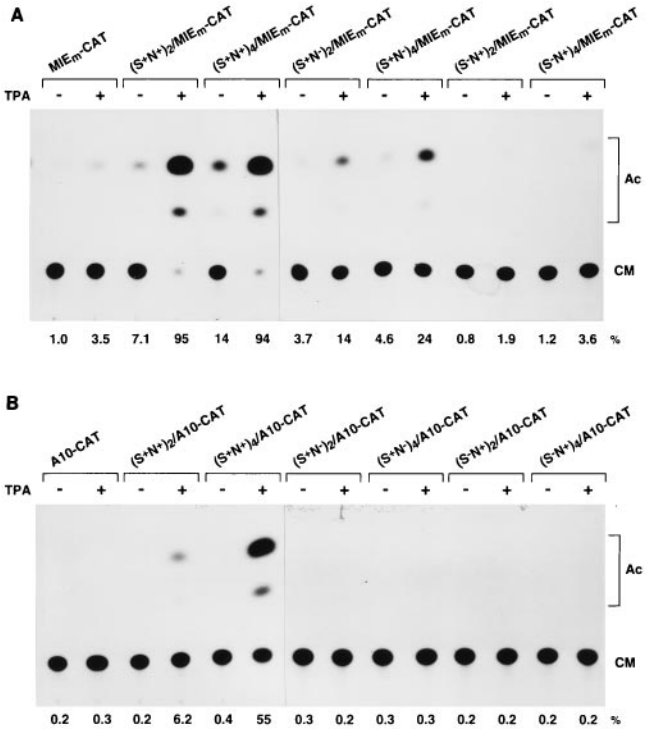

FIG. 2. (A) The S and N submotifs within the SNE consensus sequence give synergistic effects on basal enhancement and TPA responses within their natural minimal promoter context. The sample autoradiograph shows the results of a transient CAT expression assay in U-937 cells. The parent minimal SCMV(AGM) IE94(−69/+30) promoter region driving CAT reporter gene expression in plasmid pCJC81 is referred to as MIE_m-CAT; its derivatives containing a series of insertions of wild-type or mutant synthetic 30-bp SNE oligonucleotides were transfected into parallel cultures in the presence or absence of TPA and assayed for CAT activity. The $(S^+N^+)_2$/MIE_m-CAT gene (pCJC112B) and $(S^+N^+)_4$/MIE_m-CAT gene (pCJC114B) contain two and four tandem copies of the wild-type SNE motifs, respectively. The $(S^-N^-)_2$/MIE_m-CAT gene (pCJC132B), $(S^+N^-)_2$/MIE_m-CAT gene (pCJC152B), and $(S^-N^+)_2$/MIE_m-CAT gene (pCJC172B) contain two tandem copies of mutant SNE motifs with altered base pairs in the N submotif only (S^+N^-), in the S submotif only (S^-N^+), and in both the S and N submotifs (S^-N^-), respectively. Percent conversion of [^{14}C]chloramphenicol (CM) to acetylated forms (Ac) is indicated below each lane. (B) Transfer of synergistic TPA responsiveness properties to a heterologous minimal promoter background. The sample autoradiograph shows the results of similar transient CAT expression assays in extracts from U-937 cells transfected with parent plasmids containing the SV40 minimal early T-antigen promoter (pA10-CAT) and its derivatives $(S^+N^+)_2$/A10-CAT (pCJC12B), $(S^+N^+)_4$/A10-CAT (pCJC14B), $(S^-N^-)_2$/A10-CAT (pCJC32B), $(S^+N^-)_2$/A10-CAT (pCJC52B), and $(S^-N^+)_2$/A10-CAT (pCJC72B).

Effects of S and N mutations on basal enhancement and TPA responsiveness in several monocyte and lymphocyte cell types. The results with the mutant SNE oligonucleotides in the minimal SCMV MIE promoter background in U-937 cells and four other cell types, mature monocytes (THP-1), T cells (Jurkat), and both HL-60 and K-562 cells, are compared in Fig. 3A. In some cell types, we also compared the SNE results with those for parallel samples receiving similar target constructions containing two tandem repeats of wild-type and mutant forms of the SCMV series I 16-bp CRE placed in the SCMV minimal MIE promoter background, as well as with those for a classical c-Fos SRE placed in an HSV thymidine kinase promoter background. In general, basal activity for the SNE was highest in K-562 cells, in which the S^+N^- version still showed considerable activity also and the single-copy c-Fos SRE positive control gave a 22-fold TPA response. U-937 cells showed the next-highest basal levels, followed by Jurkat, HL-60, and

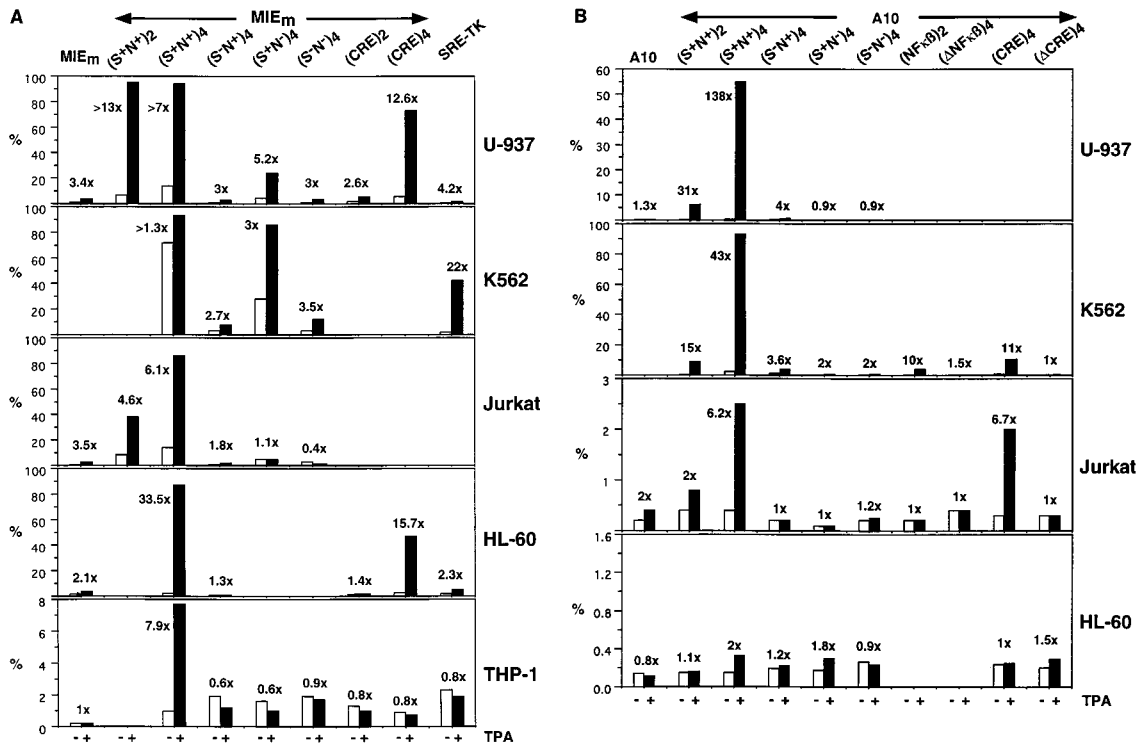

FIG. 3. (A) Comparison of the TPA responses of wild-type and mutant SNE motifs in the minimal SCMV(AGM) MIE$_m$ promoter background in five different monocyte and T-cell lines. The histogram plots the results of CAT assay measurements as direct percent conversion values. Fold induction levels for the sample pairs are shown. Open bars indicate no treatment, and solid bars denote measurements obtained after addition of TPA in parallel cultures. (B) Comparison of the TPA responses of wild-type and mutant SNE motifs in the heterologous minimal SV40 promoter background in four different monocyte or T-cell lines. The histogram plots the results of CAT assay measurements as direct percent conversion values. Fold induction values for the sample pairs are shown. Open bars represent no treatment samples, and solid bars represent plus-TPA samples.

THP-1 cells. In U-937 and HL-60 cells, the positive control 4× CREs gave 12- to 15-fold TPA responses, although the 1× c-Fos SRE now gave only a 2.5- to 4-fold stimulation; however, neither produced a detectable TPA response in THP-1 cells, whereas the 4× SNEs still gave 33- and 8-fold TPA responses in HL-60 and THP-1 cells, respectively. Note that the minimal SCMV MIE$_m$ promoter (which still has one diverged series I CRE/ATF-like motif present) contributed basal plus TPA-induced background levels of approximately 3.5-fold in both U-937 and K-562 cells. Except for this background activity, mutation of the S motif abolished essentially all SNE-mediated activity in all cell types, and mutation of the N motif considerably reduced both basal enhancement and TPA responses in U-937 and K-562 cells and abolished the responses in Jurkat, HL-60, and THP-1 cells.

The basal activities and TPA responses of the mutant SNE sites in the minimal A10-CAT reporter gene background obtained in four different cell lines are compared in Fig. 3B. Control or reference target genes containing either two tandemly repeated wild-type or mutant NFκB sites or four tandemly repeated wild-type or mutant series I CREs were also all placed into the same A10 minimal SV40 promoter background and were included in some experiments. Basal activities in the SV40 minimal promoter background were much lower than those in the MIE minimal promoter and could usually be detected only in K-562 cells. In this background, the 2× SNE motifs gave 31- and 15-fold TPA responses in U-937 and K-562 cells, which increased synergistically to 138- and 43-fold with the 4× SNE versions. This finding is comparable to 10-fold TPA effects for the 2× NFκB sites and 11-fold for the 4× CREs in K-562 cells, both of which were eliminated by specific point mutations within the core binding site motifs. Similarly, mutation of either the S or N components of the SNE motifs essentially abolished both basal (30-fold reduction in U-937 cells) and all TPA-induced activity in both cell types. In Jurkat cells, only the 4× SNE and 4× CRE targets gave any specific increase in signal after TPA treatment (six- to sevenfold each), and in both HL-60 cells (Fig. 3B) and THP-1 cells (not shown), there was no detectable activity even with TPA for any of these low basal-level target reporter genes.

The TPA response in DNA-transfected U-937 cells can be detected within 2 h and reaches at least 250-fold stimulation. To examine the time course of TPA induction mediated by the SCMV SNE sequences, we also introduced the wild-type $(S^+N^+)_4$/A10-CAT and double-mutant $(S^-N^-)_4$/A10-CAT target reporter genes into U-937 cells for 24 h and then measured the induced CAT activity in extracts prepared 1, 2, 4, 8, 12, and 24 h after TPA treatment (Fig. 4A). The control mutant target gene gave no more than 2- to 3-fold stimulation even as late as 24 h after TPA treatment, whereas the wild-type version produced greater than 20-fold induction effects at 2 h and 80-fold at 4 h, with a nearly linear response (as judged by 5- and 25-fold dilutions of the extract) for up to 24 h, reaching an overall increase of more than 1,000-fold, with a peak TPA stimulation of 250-fold at both 8 and 12 h.

From the results of all of these experiments, we can conclude, first, that the overlapping S and N submotifs are both essential for these activities and that they work synergistically in mediating transcriptional activation; second, that multimerized copies also act synergistically; third, that the response can be transferred to a heterologous promoter; and fourth, that

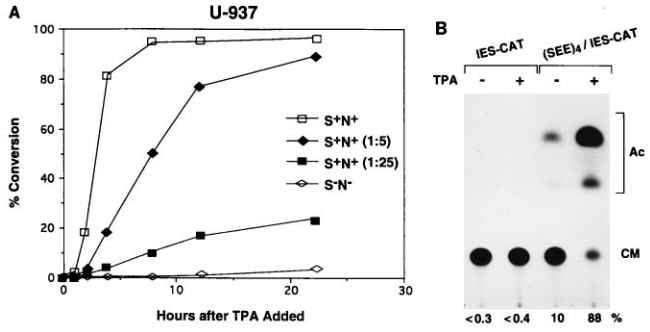

FIG. 4. (A) Time course and quantitation of TPA responsiveness of multimerized SNE motifs after transfection into U-937 cells. The $(S^+N^+)_4$/A10-CAT and $(S^-N^-)_4$/A10-CAT target genes (in plasmids pCJC14B and pCJC34B) were transfected into multiwell dish cultures, and TPA was added after 24 h. Samples were then taken for CAT assays at 1, 2, 4, 8, 12, and 22 h. Measurements were made with both the S^+N^+ and S^-N^- extracts as undiluted samples (open symbols), and the S^+N^+ extracts were also assayed at 5- and 25-fold dilution (solid symbols). (B) The analogous isolated SEE motif from the HCMV MIE_H enhancer also responds strongly to TPA induction. The sample autoradiograph shows the results of transient CAT expression assays in U-937 cells in the presence or absence of TPA, using the $(SEE)_4/IES_m$-CAT gene (pYJC384B) containing an upstream insertion of four tandem copies of the wild-type HCMV SEE motif as a synthetic 30-bp oligonucleotide (Fig. 1C) added to the parent minimal IES_m-CAT target gene (pYJC90).

significant effects can be detected as soon as 1 to 2 h after TPA treatment, making it likely that this is a direct signal transduction event rather than a process that requires prior cell differentiation.

Comparison of the basal enhancement and TPA responses of the HCMV SEE and SCMV SNE motifs in U-937 and HL-60 cells. Having obtained considerable evidence in support of a role for SRF and against the idea that NFκB/Rel factors were responsible for the TPA induction mediated by the SCMV ENH-A2 region, despite the presence of the series IIIB NFκB-like motifs, we reevaluated the possibility that the HCMV MIE enhancer has a functionally similar element. Therefore, the consensus core SRF site and surrounding sequences from positions −538 to −522 in HCMV(Towne) were synthesized as a 30-mer oligonucleotide pair, which we refer to as the SEE (Fig. 1C) because of the adjacent potential GABP/ETS class binding site and the absence of potential Rel/NFκB class motifs. To examine whether the human SEE motif behaves as a functional equivalent of the SCMV(AGM) SNE motif, we initially compared their basal enhancer activities and abilities to mediate TPA responses, using an $(SEE)_4/MIE_m$-CAT target reporter gene containing four copies of the tandemly repeated 30-bp SEE inserted into the minimal SCMV MIE_m promoter. The parent MIE_m-CAT gene and its derivatives $(SNE)_4/MIE_m$-CAT, $(SEE)_4/MIE_m$-CAT, and $(SRE)_2/MIE_m$-CAT were introduced into U-937 cells in the presence or absence of TPA and assayed for CAT activity 18 h later. The results showed that both the SNE and SEE motifs gave approximately equal TPA responsiveness but displayed different levels of basal enhancement (Fig. 5A). The $(SNE)_4$ and $(SRE)_2$ inserts both boosted the basal activity five- to sixfold in comparison with the parent MIE_m-CAT, whereas the $(SEE)_4$ insert failed to do so. However, in the presence of TPA, the activity of $(SEE)_4/MIE_m$-CAT was increased 41-fold over the basal activity, whereas the minimal MIE_m-CAT gene responded 5.7-fold. In comparison, responses of the $(SNE)_4$ and $(SRE)_2$ inserts as well as a modified $(SRE)_4$ insert containing a core RSRF binding site (CTATATATAG [68]) in place of the classical core SRF binding site (CCATATTAGG) were all beyond the linear range of the assay. However, neither the core or flanking sequence mutants of SRE gave any increased basal level or TPA responses.

In addition, we tested for SNE and SEE function in the promyelocytic leukemia cell line HL-60, which gave very low basal activity and no TPA induction with the parent minimal SCMV MIE_m-CAT gene but did demonstrate TPA responsiveness through the added elements in the $(SNE)_4/MIE_m$-CAT, $(SEE)_4/MIE_m$-CAT, and $(SRE)_2/MIE_m$-CAT genes (Fig. 5B). In this experiment, the minimal IE94 MIE_m-CAT gene responded to TPA stimulation only 1.2-fold and none of the target constructions displayed measurable increases in basal expression. In contrast, addition of four copies of the SNE and SEE motifs gave 8- and 9-fold TPA responses, respectively, which were somewhat lower than the 13-fold obtained with the wild-type $(SRE)_2$ motifs. Once again TPA induction through the HCMV $(NFκB)_4$ site or with multimerized mutant ΔSNE and ΔSRE motifs was undetectable in HL-60 cells under these conditions. Therefore, we conclude that both the SEE and SNE motifs enhance basal activity and behave similarly to each other as well as to the intact c-Fos SRE in response to TPA stimulation in both U-937 and HL-60 cell types.

Effects of spacing and substitution mutations on functions of the SNE motifs. To further dissect the molecular mechanism for synergism between the S and N submotifs in the SNE, we both altered the spacing between the two submotifs (S/InsN) and changed the series IIIB NFκB-like N submotif to a perfect classical consensus Ig kappa NFκB binding site (SNFκB). To determine whether these changes preserved the wild-type SNE function and whether NFκB was indeed involved in synergism with SRF, we tested their effects on basal enhancement and TPA responses in transient transfection CAT assays in both U-937 and HL-60 cells (Fig. 5A and B). Surprisingly, both the basal enhancement and TPA responses of the $(S/NFκB)_4/MIE_m$-CAT and $(S/InsN)_4/MIE_m$-CAT plasmids were highly impaired compared with those of $(SNE)_4/MIE_m$-CAT in U-937 cells (Fig. 5A), and the TPA responses of both altered SNEs were also virtually eliminated in HL-60 cells (Fig. 5B). Even the classical HCMV, HIV, or Ig kappa $(NFκB)_4$ insert gave no increase in basal activity and only a 2-fold boost in TPA response (from 5.7- to 13-fold) in the MIE_m-CAT background in U-937 cells and was inactive in HL-60 cells. Therefore, we conclude that it is not NFκB that is involved in the synergism with SRF to activate the SNE site. Clearly the spacing between the S and N submotifs is also important for efficient SNE function.

Lack of response of the SNE, SEE, and c-Fos SRE motifs to OA. To avoid the complications of the high basal levels, overscale responses, and three- to fivefold background TPA effects obtained with the minimal SCMV MIE_m promoter alone in U-937 cells, we also generated another set of heterologous reporter plasmids in the minimal HCMV IES(−57/+77)-CAT promoter background, which is associated with the IES enhancer control region regulating the HCMV US3 gene (8). In this case, four copies of the wild-type SEE oligonucleotide increased the basal activity 33-fold and gave an additional 9-fold stimulation after TPA treatment in U-937 cells, whereas the parent minimal HCMV IES_m-CAT plasmid gave neither significant enhancement of basal levels nor any TPA responsiveness (Fig. 4B).

We have demonstrated previously that, unlike the intact enhancer/promoter region in the HIV LTR, HCMV MIE_H, and HCMV IES (US3) genes, the intact SCMV enhancer/promoter region from positions −633 to +30 fails to respond either to tumor necrosis factor alpha (TNF-α) or to OA in U-937 cells (8, 11). To examine whether this finding represented a difference between the isolated multimerized SNE,

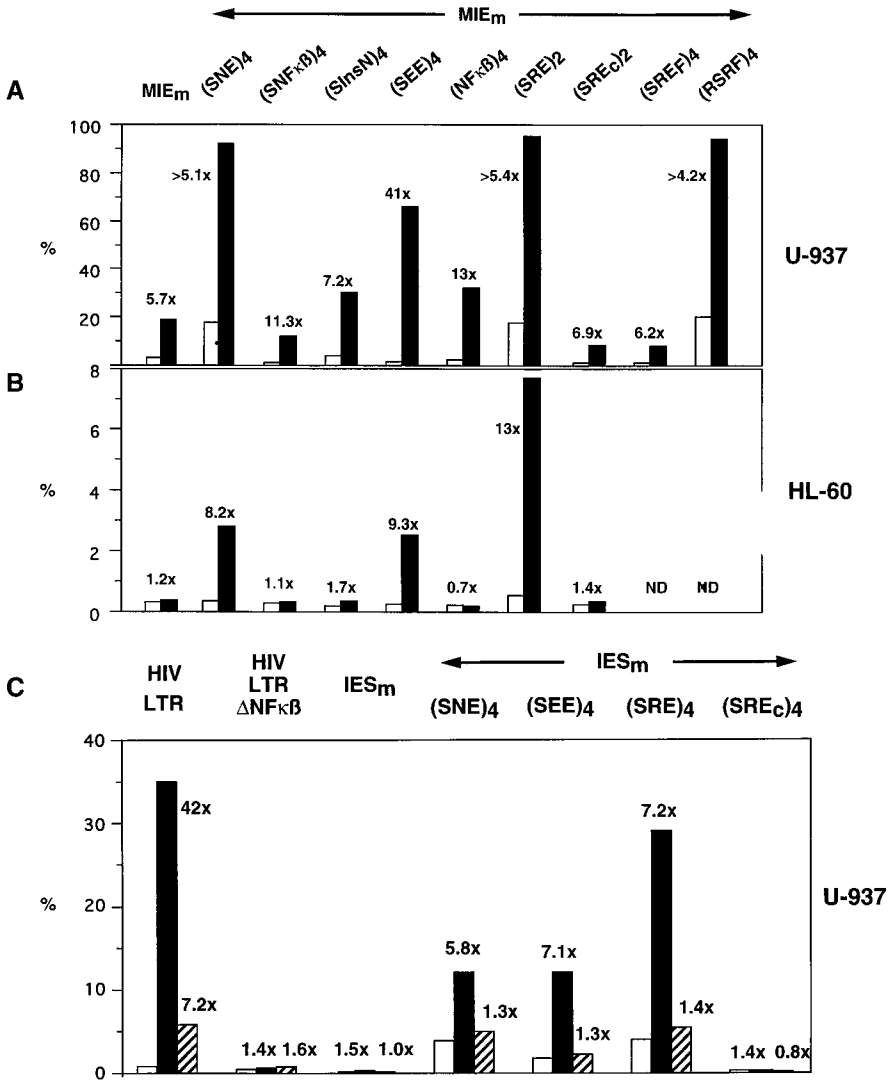

FIG. 5. (A and B) Evidence that NFκB is not involved in synergism with SRF and that the spacing between the S and N motifs is critical for synergism. The histograms show the results of transient CAT expression assays in U-937 cells (A) or HL-60 cells (B) with the parent SCMV(AGM) minimal MIE_m-CAT gene (pCJC81), or versions containing upstream insertions of four tandem copies of the SNE oligonucleotide motif from the SCMV(AGM) MIE_s enhancer, to generate the $(SNE)_4/MIE_m$-CAT gene (pCJC114B), a version with the classical Ig kappa NFκB motif substituted for the N submotif in $(S/NF\kappa B)_4/MIE_m$-CAT (pYJC224B), a 2-bp insertion mutant between the two submotifs in $(S/InsN)_4/MIE_m$-CAT (pYJC244B), and the HCMV SEE motifs in the $(SEE)_4/MIE_m$-CAT gene (pYJC294B). Other control and mutant target constructions include four copies of the HCMV MIE_H consensus NFκB site in $(NF\kappa B)_4/MIE_m$-CAT(pYJC304), two copies of the c-Fos wild-type SRE in $(SRE)_2/MIE_m$-CAT (pYJC262), two copies of the c-Fos SRE flanking ETS sequence mutant $(SRE_c)_2/MIE_m$-CAT(pYNC282), four copies of the c-Fos SRE core SRF point mutant in $(SRE_F)_4/MIE_m$-CAT (pYJC324), and four copies of a c-Fos SRE variant containing an RSRF core binding site in $(RSRF)_4/MIE_m$-CAT (pYJC314). ND, not determined. Samples were either untreated (open bars) or treated with TPA (solid bars). Results are plotted as percent conversion of [^{14}C]chloramphenicol to acetylated forms, and fold induction values are indicated for the sample pairs. (C) Unlike the HIV NFκB motifs, the SNE, SEE, and SRE motifs do not respond to OA stimulation U-937 cells. The histogram shows the TPA and OA responsiveness in U-937 cells of the parent minimal nonresponsive $IES(-54/+80)$-CAT gene (=IES_m-CAT in pYJC90) or versions containing four added tandem copies of the wild-type SCMV SNE motif in the $(SNE)_4/IES_m$-CAT gene (pYJC794B), the wild-type HCMV SEE motif in the $(SEE)_4/IES_m$-CAT gene (pYJC384B), the wild-type c-Fos SRE motif in the $(SRE)_4/IES_m$-CAT gene (pYJC414B), and a c-Fos core SRE motif only containing point mutations in the flanking ETS binding site $(SRE_c)_2/IES_m$-CAT gene (pYJC282A). The wild-type HIV LTR-CAT gene (in plasmid pU3RIII) and a derivative with the NFκB sites mutated as the LTR(ΔNFκB)-CAT gene (mpU3RIII) were used as controls. Parallel cultures were grown in the presence of 50 ng of TPA per ml or 25 nM OA or in the absence of both and harvested for CAT assays. Measurements are plotted as percent conversion, and fold induction values are shown. Open bars, no treatment; solid bars, plus TPA; hatched bars, plus OA.

SEE, or SRE motifs and the classical Ig kappa-like NFκB binding sites that are present in all three of the other enhancers, we compared the TPA and OA responses among CAT reporter genes containing the parent minimal HCMV IES promoter (IES_m-CAT) with four copies of the SCMV SNE, HCMV SEE, c-Fos SRE, or c-Fos core SRF motif added in a transient DNA transfection assay in U-937 cells (Fig. 5C). As expected, the minimal promoter in IES-CAT failed to respond to either TPA or OA, whereas the basal CAT enzyme levels increased 19-fold with the $(SNE)_4/IES_m$-CAT gene, and TPA stimulation gave an additional 6-fold boost in activity. In contrast, OA stimulation gave only a 1.3-fold increase over basal levels. Similarly, $(SEE)_4/IES_m$-CAT displayed a 9-fold increased basal level and responded 7-fold to TPA but not to OA (1.3-fold increase). The $(SRE)_4/IES_m$-CAT gene behaved essentially the same as our SEE and SNE targets by giving 20-fold increased basal CAT enzyme levels and a 7-fold TPA response but only a 1.4-fold OA response. Both effects were

lost by mutation of the flanking ETS motif in the SRE. In comparison, although no significant OA responses were observed with any of the three SRF-containing elements, the same concentration of OA stimulated the wild-type HIV LTR-CAT control target containing two intact classical NFκB sites sevenfold in parallel assays but had no effect on the HIV LTR(ΔNFκB)-CAT mutant version in which both NFκB sites were mutated (Fig. 5C). Similar results have also been obtained with 2× tandemly repeated wild-type and mutant NFκB sites placed upstream of the SV40 minimal promoter in the A10-CAT gene (not shown). Therefore, we conclude that all three SRF-containing elements respond to signal transduction pathways generated by TPA stimulation (presumably predominantly by PKC pathways) but that unlike NFκB motifs, they do not respond to OA at concentrations that are known to inhibit phosphatase 2A (PP2A) activity and subsequent IκB degradation.

Identification of specific cellular factors that bind to the SNE motifs in U-937 and Raji nuclear extracts. The 67-kDa SRF protein ($p67^{SRF}$) was identified as a constitutively expressed cellular DNA-binding protein that specifically recognizes the core motif, CCATATTAGG, within the c-Fos SRE sequence (56, 83). SRF also forms a ternary complex with an ETS family protein, $p62^{TCF}$ (now known as ELK-1 or SAP-1), which recognizes the flanking sequence (C/A)(C/A)GGA (T/A) located 2 bp 3′ to the c-Fos core SRF binding site and has been thought to be required for full serum response activity (24, 52, 63, 66, 69). Note that ELK-1 and SAP-1 do not bind stably to this sequence on their own. Since both the SNE and SEE motifs also contain consensus core ETS binding motifs (GGAA), although their flanking sequences differ significantly from those of the c-Fos SRE site, we needed to know what cellular factors might be involved in binding to the N or E submotif to generate the synergistic TPA response effects with the S submotif.

We showed previously that a 30-bp SNE oligonucleotide probe from the SCMV MIE ENH-A2 region bound to cellular SRF by EMSA using a partially purified heparin-agarose fraction from a Raji cell nuclear extract that contains SRF binding activity (10). However, in retrospect it was not clear whether this represented just SRF or a potential SRF-ETS ternary complex. Therefore, in an initial experiment with the same Raji cell fraction, a control ^{32}P-labeled classical c-Fos SRE oligonucleotide probe was compared with both wild-type and mutant forms of the SNE probe (Fig. 1C). The wild-type SNE probe as well as the N submotif mutated SNE oligonucleotide probe (SΔN) both formed single complexes migrating at the same position as the wild-type SRE oligonucleotide probe (Fig. 6A, lanes 1 to 3). However, a probe with mutations in both the S and N submotifs (ΔSΔN; lane 4) failed to generate a shifted band at the same position. Evidently, partially purified Raji SRF can form a direct protein-DNA complex with the wild-type SNE that lacks any ETS protein component and is indistinguishable from that of the SRF binary complex formed on the SRE. Formation of this binary complex is also independent of the presence or absence of the flanking series IIIB N motif or core ETS motifs in the SNE probe.

To look for potential additional specific SNE-binding proteins in U-937 cells, we also performed EMSAs using a more extensive series of synthetic 30-bp oligonucleotides derived from the wild-type SCMV SNE sequence (Fig. 1C). The wild-type SNE probe formed the classical SRF complex with unfractionated U-937 nuclear extracts, together with both a slower-mobility band (C complex) and a faster-mobility band (YY1 [not shown]) (Fig. 6B, lane 1). The YY1 complex will be described elsewhere, but its binding pattern does not correlate directly with TPA responsiveness (1). As expected, the SRF submotif mutant ΔS/N probe (lane 2) was not able to form either the SRF, YY1, or C complex, but the series IIIB/ETS submotif mutation in the S/ΔN probe prevented formation of only the ternary C complex, with a concomitant large increase in the abundance of the binary SRF complex (lane 3). The double-mutant probe, ΔS/ΔN, failed to form any of these three DNA-protein complexes but did produce a new, presumably nonrelevant bound species (X) that was not seen with any other probe (lane 4). The mutant S/NFκB probe, which was modified in its flanking sequences to mimic the Ig kappa classical NFκB binding sequence, again gave a high level of binary SRF complexes but failed to form any C complex (lane 5). On the other hand, the mutant S/InsN probe, which contained intact SRF and ETS submotifs but with two extra base pairs inserted to change the spacing between them, still formed the C complex although at reduced efficiency (lane 6). Therefore, we concluded that the C complex must consist of both SRF and a second, unknown factor that is not NFκB-related and that both proteins might be involved in mediating the synergism between the S and N submotifs in enhancing the basal transcriptional activity and conferring TPA responsiveness.

Analysis of the SEE and SRE motif-binding factors by competition EMSAs. Although SRF DNA-protein complexes formed efficiently on the SNE motif, formation of the direct binary complex could not be responsible for the inducible enhancer properties of the SNE or SEE because the S/ΔN probe, which failed to give normal levels of basal enhancement and TPA responses, still formed the binary SRF complex with high efficiency (Fig. 6A and B, lanes 3). Similar conclusions were derived by others from c-Fos SRE studies, indicating that SRF is necessary, but not sufficient, both for ternary complex formation and for mediating serum and TPA responses (26, 69, 83). Comparison of the flanking sequences in the SRE, SEE, and SNE reveals little homology except for a GGA(A/T) motif (Fig. 1B), which represents a common core element recognized by many ETS family proteins such as GABP, ETS-1, ETS-2, PEA3, SAP-1, ELK-1, and PU1 (38, 51). Since the flanking sequence of the SEE motif resembles a perfect GABP binding site, GCGGAAC (43), and it is known that both the ELK-1 and SAP-1 ETS class proteins can form ternary complexes with SRF on the c-Fos SRE site (15, 30, 66), we were interested in knowing whether these or any other ETS family proteins could form complexes with SRF on our SEE or SNE motif.

Therefore, to test whether the C complex contains both ETS family proteins and SRF, competition EMSAs were performed with either the SNE, SEE, or SRE oligonucleotide pairs as probes and nuclear extracts from U-937 or HeLa cells. Both the SNE and SEE probes formed the typical SRF and ternary C complexes with HeLa cell extracts (Fig. 6C, lanes 1 and 4). In the presence of an excess of the oligonucleotide containing the core SRF binding site only, both the binary SRF and C complexes were abolished, whereas with an excess of the oligonucleotides containing three adjacent copies of the wild-type core GABP binding sites as a competitor, formation of only the C complex was abolished from the HeLa cell extract (Fig. 6C, lanes 2 and 5) and (particularly for SEE) the intensity of the binary SRF band increased (Fig. 6C, lanes 3 and 6). The same change in pattern with the 3× GABP competitor was observed for both the SEE and SRE probes with U-937 extracts (Fig. 6D, lanes 2, 3, 10 and 11). In contrast, the mutant GABP oligonucleotide probe 3× ΔGABP was not able to compete with C-complex formation (lanes 4 and 12). An excess of unlabeled oligonucleotides containing just a single GABP core motif 1× GABP also consistently reduced SNE C-complex formation, although to a lesser degree than with 3× GABP

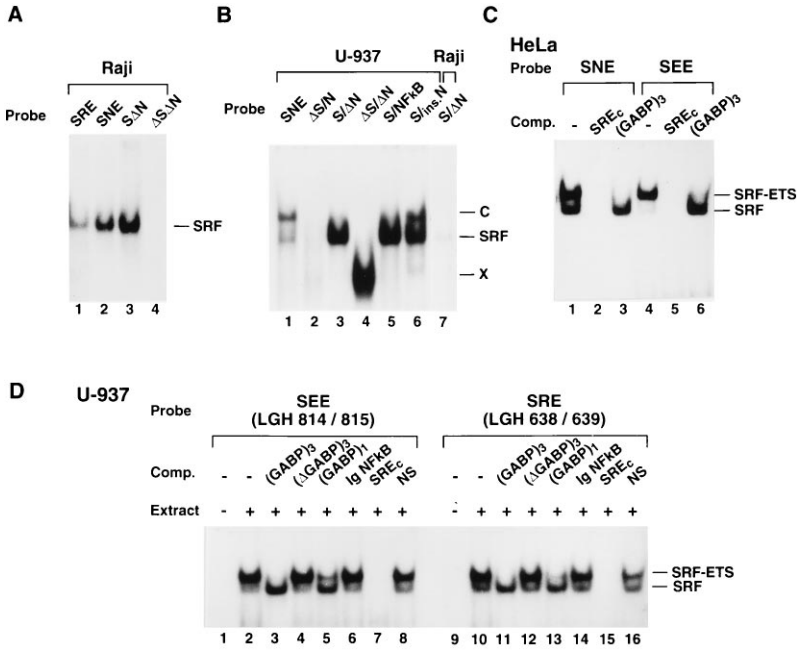

FIG. 6. Demonstration of SRF and ETS protein binding to the SNE and SEE probes. (A) EMSA results showing binding of Raji cell SRF protein to both the c-Fos SRE and the SCMV SNE core sequences. A pool of fractions from heparin-agarose chromatography of a Raji cell nuclear extract previously shown to contain SRF activity was incubated with ^{32}P-labeled 30-bp oligonucleotide probes representing the wild-type c-Fos SRE motif (LGH638/639; lane 1), the wild-type SCMV SNE motif (LGH218/219; lane 2), the N submotif mutated SNE site (LGH324/325; lane 3), or the S and N submotif double-mutated SNE site (LGH322/323; lane 4). SRF refers to the core SRF-bound complex. Only the relevant upper portion of the gel is shown. (B) Detection of novel SNE-specific DNA-protein complexes in unfractionated U-937 nuclear extracts. Total U-937 nuclear extracts were used in an EMSA with a series of ^{32}P-labeled oligonucleotide probes representing the wild-type SNE motif (lane 1), the S submotif mutated SNE site (ΔS/N, LGH399/400; lane 2), the N submotif mutated SNE site (S/ΔN, LGH324/325; lane 3), the S and N double-mutated SNE site (ΔS/ΔN, LGH322/323; lane 4), the classical NFκB modified SNE site (S/NFκB, LGH801/802; lane 5), and the SNE site with a 2-bp insertion (S/InsN, LGH803/804; lane 6). A partially purified Raji cell extract fraction was used to show the position of a core SRF complex (lane 7). C refers to a tripartite SRF-ETS complex found in the U-937 cell extract but not in the Raji extract fractions. X indicates a nonrelevant artifactual binding factor associated with the SNE(ΔS/ΔN) double mutation. (C) Demonstration that the slowly migrating C band represents a tripartite SRF-ETS class protein complex. EMSA results using an unfractionated HeLa cell extract with ^{32}P-labeled wild-type SCMV SNE (LGH218/219) and HCMV SEE (LGH814/815) oligonucleotide probes. Control lanes received added protein extract and poly(dI-dC) but without specific competitor (Comp.; lanes 1 and 4). Unlabeled 30-bp annealed oligonucleotides were added as competitor DNA in 300-fold molar excess over the probe DNA. These included either the c-Fos core SRE motif with the core c-Fos SRF binding site intact, but the adjacent ETS motif mutated (SRE_c, LGH642/643; lanes 2 and 5), or three copies of the wild-type GABP motif from the HSV IE175 promoter [$(GABP)_3$, LGH663/807; lanes 3 and 6]. (D) Similarity of the HCMV SEE binding pattern to that of the c-Fos SRE. Competition EMSA results using U-937 nuclear extracts and ^{32}P-labeled oligonucleotide probes representing the wild-type HCMV SEE motif (LGH814/815) or the wild-type c-Fos SRE motif (LGH638/639). Where indicated, unlabeled annealed oligonucleotides were added as competitor DNA (300-fold excess); these contained the wild-type $(GABP)_3$ sites (LGH663/807; lanes 3 and 11), mutant $(\Delta GABP)_3$ sites (LGH665/666; lanes 4 and 12), a single copy of the wild-type $(GABP)_1$ site (LGH808/809; lanes 5 and 13), the wild-type Ig kappa NFκB site (LGH816/817; lanes 6 and 14), the c-Fos core SRF binding sites (SRE_c, LGH642/643; lanes 7 and 15), or a nonspecific (NS) 30-bp sequence (LGH531/532; lanes 8 and 16). Control lanes received either no protein and no competitor DNA (lanes 1 and 9) or added protein and poly(dI-dC) without specific competitor DNA (lanes 2 and 10). F, free probe; SRF, bound core SRF-bound DNA complex; SRF-ETS, bound tripartite complex containing SRF and an ETS-like protein.

(lanes 5 and 13). Importantly, oligonucleotides representing the wild-type classical Ig kappa NFκB binding sites (Ig NFκB), which incidentally also contains GGAA in the sequence, had no effect on C-complex formation (lanes 6 and 14). However, competitor oligonucleotides containing only the core SRF binding site (CCATATTAGG) (SRE_c; lanes 7 and 15) once again completely abolished the formation of both the binary SRF and C complexes with the U-937 extract. A control irrelevant oligonucleotide competitor at the same concentration also failed to affect complex formation (lanes 8 and 16). Note that almost exactly the same overall patterns of complex formation and competition were observed when the c-Fos SRE oligonucleotide pair was used as an EMSA probe compared with the SEE probe (Fig. 6D).

Because of the presence of common core GGAA-like recognition sequences for all ETS class proteins, it was not possible to determine from these experiments whether GABP itself forms the ternary C complex with SRF on the overlapping SRF-ETS site in the SEE probe. Perhaps any ETS family protein, including SAP-1 or ELK-1, can be competed by the GABP binding sites in a semispecific manner. GABP itself usually binds stably only as an α-β heterodimer to two adjacent core GCGGAAC-like motifs. However, it appeared very likely that some ETS class family protein formed the tripartite C complex together with SRF, whereas SRF alone produced the faster-migrating binary SRF complex. Evidently, in the presence of excess competing core ETS binding sites, C-complex formation was disrupted and SRF was released from the ternary complex to form more of the direct binary SRF complex.

Relative abundance of SRF and SRF-ETS complexes in different cell types. To determine whether the SRF and associated ETS class proteins that bind to the SEE and SNE probes show a cell-type-specific distribution pattern, we performed EMSAs using ^{32}P-labeled probes with nuclear extracts from different cell types. The results showed that SRF was present in every cell type tested (Fig. 7A, lanes 1 to 9), but its amount varied (low in Raji and Vero cells). In addition, the SRF-ETS C complex was not found in HF, Raji, BALB/c 3T3, or Vero cells by EMSA, although both the SRF and SRF-ETS C complexes were present at approximately equal levels in U-937, K-562, HeLa, and HL-60 cells. Furthermore, there appeared to be a significant increase (approaching twofold) in the ratio of ternary SRF–ELK-1 complexes compared with binary SRF

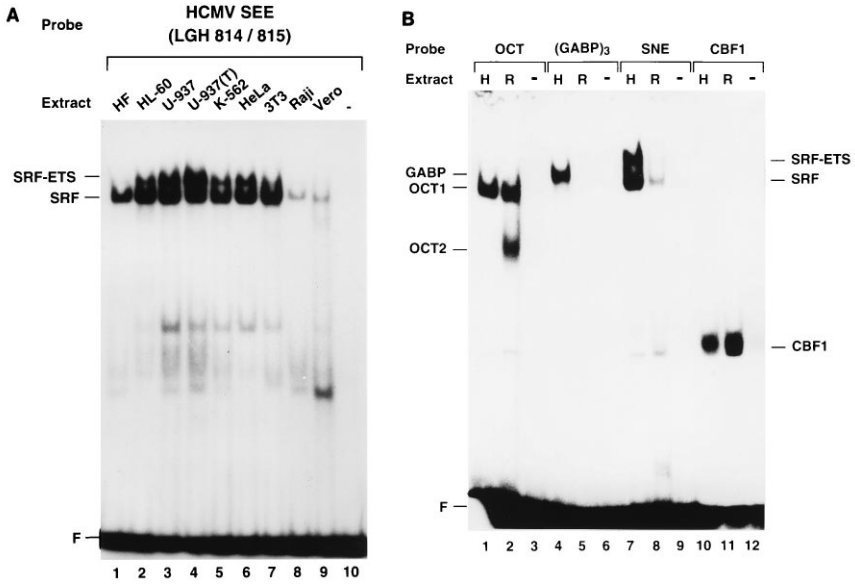

FIG. 7. Differences in cell-type-specific distribution of the SRF and ETS factors. (A) Preferential distribution of SRF-ETS complexes in myeloid cell types compared with HF and BALB/c 3T3 cells. The autoradiograph shows results of EMSA using the ^{32}P-labeled wild-type SEE probe (LGH814/815) and different nuclear extracts. Lanes: 1, HF cells; 2, HL-60 cells; 3, U-937 cells; 4, U-937 cells stimulated with TPA (50 ng/ml) for 18 h; 5, K-562 cells; 6, HeLa cells; 7, BALB/c 3T3 cells; 8, Raji cells; 9, Vero cells. Control lane 10 received ^{32}P-labeled probe DNA without any added sample protein. F, free probe; SRF, core SRF-bound DNA complexes; SRF-ETS, tripartite DNA complexes. (B) Selective absence of GABP and SRF from Raji cell extracts compared with HeLa extracts. The autoradiograph compares the patterns of binding to four transcription factor site probes in unfractionated HeLa (H) and Raji (R) cell nuclear extracts. The probes used (all 30-mer oligonucleotide pairs) represented classical OCT sites (LGH49/50; lanes 1 to 3), the HSV triple GABP sites (LGH663/807; lanes 4 to 6), the SCMV wild-type SNE sites (LGH218/219; lanes 7 to 9), and the Epstein-Barr virus EBNA2 promoter site CBF1 (LGH941/942; lanes 10 to 12). The third lane in each set represents a no extract control.

complexes bound to the SEE probe in 18-h TPA-treated extracts relative to that in untreated U-937 nuclear extracts (compare lanes 3 and 4).

For further evaluation of the apparent large differences between HeLa and Raji cells, we also compared the patterns of protein binding to four different oligonucleotide probes (OCT, GABP, SNE, and CBF1), using total unfractionated HeLa and Raji cell nuclear extracts (Fig. 7B). The results revealed that although the unfractionated Raji B-lymphocyte sample contained just as much or more OCT-1 (lanes 1 and 2) and CBF-1 (lanes 11 and 12) as were present in the HeLa cell extract (as well as a B-cell-specific OCT-2 band; lane 2), it was totally devoid of GABP binding activity (lane 5) and formed only very limited amounts of an SNE-bound SRF band (lane 8), which did not include any detectable SRF-ETS C-complex. Therefore, we conclude both that the amount of SRF varies in different cell types and that the particular ETS protein involved shows a highly cell-type-specific distribution that does not include Raji, HF, BALB/c 3T3, or Vero cells.

Antibodies specific to several ETS family proteins fail to recognize the SNE protein complex. ETS family proteins consist of at least seven distinct members that have similar DNA binding domains (with the common core target recognition motif GGAA or GGAT), but they differ greatly in structure over the remaining domains of each protein (67). To attempt to determine definitively which member of the ETS family may be involved in synergism with SRF, we performed supershift EMSAs with specific antibodies added to the complexes formed by U-937 and HeLa nuclear extracts with the SEE, SNE, and SRE probes. Since the SEE flanking sequences closely resemble the GABP binding site, we also wanted to determine whether GABP might itself be involved in forming C complexes with SRF. First, we used our control triple-motif GABP binding site probe from the HSV IE175 promoter to determine whether U-937 cells express GABP. In the absence of any antibody, U-937 nuclear extracts formed a predominant relatively fast-migrating band with the 3× GABP probe (Fig. 8A, lane 1). This band was totally supershifted by either anti-mouse GABPα or anti-mouse GABPβ rabbit polyclonal antiserum (lanes 2 and 3). However, other antisera recognizing different members of the ETS family such as the ETS-1, ETS-2, PEA3, and PU1 proteins all failed to supershift the GABP complex (lanes 4 to 7). Therefore, U-937 cells do contain both GABPα and GABPβ. However, with U-937 extracts, neither the SRF-ETS C complex that formed on the SEE site probe nor that formed on the c-Fos SRE site probe was supershifted by any of the antisera tested, including GABPα and -β (Fig. 8B).

We also tested HeLa cell nuclear extracts with both the SEE and GABP probes to determine whether HeLa cells also contain GABP and whether GABP or other known ETS class proteins form complexes with SRF. Again, the 3× GABP probe bound to factors present in the extract and was supershifted by anti-GABPα antibodies (Fig. 8C, lane 2) but not by the anti-ETS-1, anti-ETS-1/2, or anti-PEA3 antibodies, whereas the C complexes formed with the SEE probe failed to be affected by any of the antibodies tested.

ELK-1 but not GABPα forms ternary complexes with SRF on both the SEE and SNE motifs. Although the flanking sequences of the SEE and SNE motifs do not closely resemble those of the c-Fos SRE, and the SNE sites do not mediate serum responsiveness, it still seemed plausible that ELK-1 or SAP-1 might recognize these atypical sequences (33). Therefore, to determine whether the ELK-1 protein formed a ternary complex with SRF on the SEE or SNE site, we performed an additional set of supershift EMSAs in agarose gels with the anti-mouse GABPα and anti-human ELK-1 rabbit polyclonal antisera, using U-937 nuclear extracts and the ^{32}P-labeled $(GABP)_3$, SEE, and SRE oligonucleotide probes. Control experiments showed that the appropriate anti-GABPα and anti-

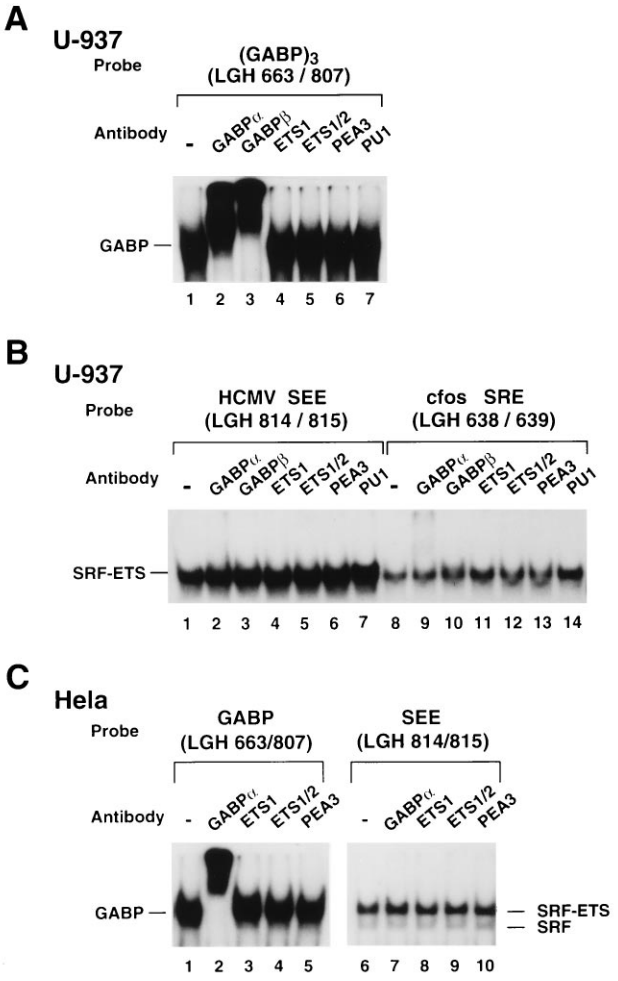

FIG. 8. Antibody supershift assays fail to detect GABP or several other ETS family proteins in the SRF-ETS complexes. (A) Only anti-GABP antibodies supershift the standard GABP complex from U-937 cells. Nuclear extracts were incubated with the ^{32}P-labeled wild-type triple $(GABP)_3$ site probe (LGH663/807) in the presence of antibodies against different ETS family members (GABPα, GABPβ, ETS-1, ETS-1/2, PEA3, and PU1). The control (lane 1) received added protein sample without any antibody. (B) Similar antibody supershift experiments using U-937 nuclear extracts and the ^{32}P-labeled single-copy wild-type HCMV SEE motif (LGH814/815) and wild-type c-Fos SRE motif (LGH638/639) probes. Control lanes 1 and 8 received added protein sample without any antibody. (C) Similar antibody supershift using HeLa cell nuclear extracts and the ^{32}P-labeled wild-type $(GABP)_3$ and HCMV SEE probes. Note that only the relevant upper parts of the polyacrylamide gels are shown.

ELK-1 antibodies specifically supershifted either the GABP or the SRF–ELK-1 complexes on the IE175 3× GABP and c-Fos SRE site probes, respectively (Fig. 9A, lanes 4 and 18). Furthermore, the SRF-ETS C-complex formed on the HCMV SEE probe was also totally supershifted by the ELK-1 antibody but not by the GABPα antibody (lanes 10 and 12). Therefore, we conclude that in the U-937 cell extracts, ELK-1 does associate with bound SRF efficiently to form the ternary C complex on the HCMV SEE probe, as well as on the c-Fos SRE probe. Importantly, control samples containing free probes plus antibodies only did not show any nonspecific bands (lanes 3, 5, 9, 11, 15, and 17).

To determine whether the SRF-ETS complex that recognized the SCMV SNE site also contained the ELK-1 protein, we performed similar supershift EMSAs using both the SEE and SNE probes and the U-937 cell nuclear extract. Indeed the anti-ELK-1 antibody proved to supershift the SRF-ETS C complexes on both the SEE and SNE probes (Fig. 9B, lanes 4 and 8). Again, the control lanes with free probes plus antibodies did not show any nonspecific DNA-binding activity (lanes 2 and 6). However, in contrast to the totally supershifted SRF-ETS complex obtained with the SEE probe, only part of the tripartite SRF-ETS C complex obtained with the SNE site probe was supershifted in the presence of the ELK-1 antibody. Instead, the amount of unassociated SRF protein that bound to the core SRE site as the binary SRF complex was increased (Fig. 9B; compare lanes 7 and 8). These results suggest that ELK-1 antibody interferes with the ternary SRF–ELK-1 complex on the SNE motif, whereas it produced a stable bound antibody–SRF–ELK-1–DNA complex on the SEE motif. Since there are differences between them in the relative spacing of the core SRF and ETS motifs (i.e., 2 bp in SEE sites but 3 bp in the SNE sites [Fig. 1B]) as well as differences in the sequences of the core SRF binding motifs compared with the c-Fos SRE, we suggest that the conformations of the SRF–ELK-1 complexes on the SEE and SNE sites may be somewhat different (Fig. 10).

DISCUSSION

Role of the PKC pathway in activating CMV MIE genes. Since regulation of the HCMV MIE enhancer/promoter directly influences both expression of the IE1 and IE2 mRNAs and the subsequent effects of the IE1 and IE2 proteins on progression of the viral lytic cycle, it is presumed to provide the major switch point leading into and out of latency and the lytic cycle. Therefore, a full understanding of HCMV MIE gene regulation is expected to both offer major insights into CMV biology and allow for its more effective use in gene therapy procedures in the future. An early model involving mouse CMV latency demonstrated that the virus lytic cycle could be reactivated from quiescently infected mouse monocytes after differentiation into macrophages (17). However, the cell types involved in reactivation and latency for primate CMVs have not yet been unambiguously identified. Certainly, differentiated macrophages can be permissive for HCMV infection (19, 32, 46, 79), and since monocytes from healthy HCMV carriers harbor PCR-detectable CMV genomes without expressing IE gene products, they are suspected of being a primary site of HCMV latency also (39, 71, 78). Several studies have demonstrated that TPA stimulation can differentiate HL-60 promyelocytic cells or U-937 histiocytic leukemia cells into macrophage-like cells (27, 77, 86) as well as induce both the HIV LTR and HCMV MIE promoter/enhancer regions (11, 53, 64). These processes are generally anticipated to involve induction of NFκB by release from IκB inhibition and can be mimicked with TNF-α (18, 73) or abolished by mutation of target NFκB binding sites in the LTR (3, 53). Nevertheless, we have demonstrated that TPA stimulation also strongly activates the SCMV MIE enhancer through other motifs that include both the multiple CREs in the ENH-A1 region and the SNE motifs in the ENH-A2 region in a variety of lymphocyte and monocyte cell lineages (11). As shown here, the SNE-mediated effect occurs within 2 h of addition of TPA to U-937 cells, which suggests that it can involve a direct signal transduction event without requiring prior differentiation events. Another cell culture induction model has shown that nonpermissive human teratocarcinoma stem cells can become permissive to HCMV infection after differentiation by RA (23, 40). In both cases, the differentiation signal not only changes the cellular status but also appears to directly potentiate viral gene expression (21).

Overall, the results of our studies as summarized in Fig. 11 have now clearly defined the mechanism of a third distinct PKC-targeted TPA response pathway, which involves the SRF-

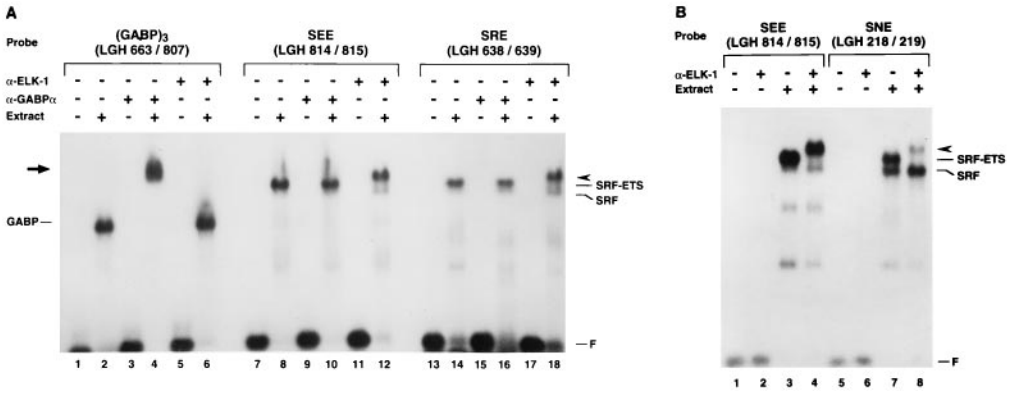

FIG. 9. Antibody supershift assays demonstrate that ELK-1 protein is present in both the HCMV and SCMV SRF-ETS complexes. (A) EMSA results showing that anti-ELK-1 antibodies supershift the SRF-ETS complex on the SEE site. U-937 nuclear extracts were incubated with the ^{32}P-labeled wild-type $(GABP)_3$ probe (LGH663/807; lanes 1 to 6), HCMV SEE probe (LGH814/815; lanes 7 to 12), and wild-type c-Fos SRE probe (LGH638/639; lanes 13 to 18) in the presence or absence of anti-GABPα or anti-ELK-1 antibodies. The control lanes received added antibodies without protein samples (lanes 3, 5, 9, 11, 15, and 17) or received added protein samples without antibodies (lanes 2, 8, and 14). (B) Similar antibody supershift experiments using U-937 nuclear extracts and the ^{32}P-labeled wild-type HCMV SEE probe (LGH814/815) and SCMV SNE probe (LGH218/219). The controls received added protein sample without any antibody (lanes 2 and 6) or received added antibodies without protein samples (lanes 3 and 7). F, free probe.

binding and c-Fos SRE-related SCMV SNE and HCMV SEE motifs that are likely to contribute to regulation of the MIE enhancers of HCMV and SCMV (Fig. 12). Several reports have focused previously on the isolated multicopy CRE (19-bp) elements that are common to all primate CMV MIE enhancers and revealed their ability to respond to cAMP inducers (9, 31, 72), or to phytohemagglutinin plus phorbol myristate acetate in T cells (31, 55), as well as directly to TPA treatment in U-937, K-562, and HL-60 cells (11). Similarly, the multicopy classical NFκB elements present in the human MIE and IES enhancers (but not in the simian MIE enhancer) were found to respond to TPA (11, 64) as well as to TNF-α (11). Note that there are also several consensus AP-1 sites in the human and chimpanzee CMV MIE enhancers that are also likely to respond to TPA, as well as several possible diverged AP-1-related sites in the circopithecoid simian versions, but none have been studied directly. Although we have been unable to demonstrate any serum responsiveness of the SCMV ENH-A2 region or by multimerized SNEs in either BALB/c 3T3 or NIH 3T3 cells (10, 11), there are many other potential core SRE- and RSRF-like motifs in all primate CMV extended MIE control regions (although usually without overlapping ETS motifs), and therefore the possibility of serum responsiveness under other circumstances or through the SEE motifs remains (Fig. 10).

Evidence against the possibility of a role for NFκB family proteins (5, 80) in the TPA responses of the SNEs comes from several sets of results. First, there was a decrease in activity

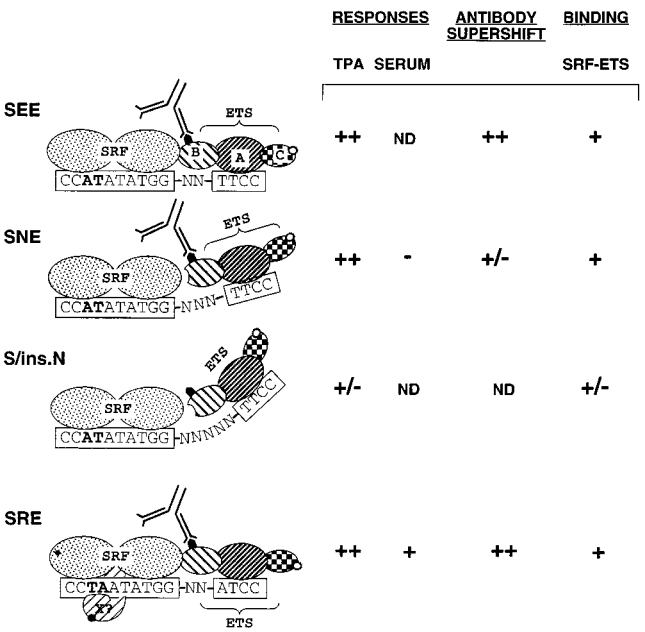

FIG. 10. Spatial and conformation effects of SRF-ETS interactions. The model shows the spatial relationship between the SRF and the ETS class ELK-1 protein binding sites on the four SRE-related motifs indicated at the left. Also shown are their responses to TPA and serum induction and their abilities to bind to the SRF-ETS complex and to form ELK-1 antibody-supershifted complexes. The ELK-1 protein contains three conserved regions designated domains A (for DNA binding), B (for SRF interaction), and C (for regulation by phosphorylation). Note that the spaces between the SRF and ETS binding sites (boxed) are 2 bp in the SEE and SRE motifs but 3 bp in the SNE motif. The spatial effects might explain the antibody supershift results. Boldface letters indicate sequence differences among the core SRF motifs within the SEE, SNE, and SRE motifs. This A/T-rich core appears to be important for a putative unknown factor (X) that mediates serum responsiveness (28). ND, not determined.

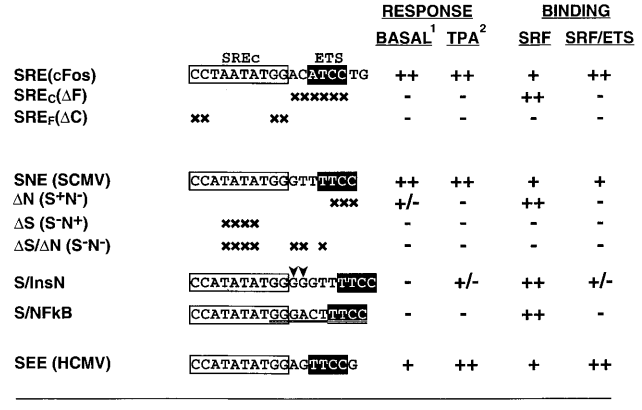

FIG. 11. Correlation between formation of SRF-ETS complexes and functions of SNE-related elements. ×, position of mutated nucleotides.

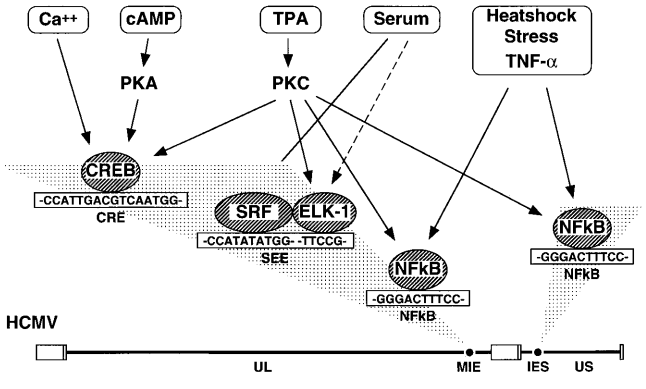

FIG. 12. Signal transduction pathways and HCMV IE gene regulation. The diagram shows several different pathways (arrows) and their target cellular mediator proteins (circled), together with the consensus DNA recognition sequences that are known to participate in the control of HCMV IE gene transcription. MIE and IES refer to the two distinctive HCMV IE enhancers that drive expression of the transcripts that encode the IE1 and IE2 (MIE) or the US3 (IES) proteins, respectively. Different stimulants (rectangles) activate different pathways. The dashed lines indicate uncertainties.

obtained when the NFκB-like series IIIB submotif (N) was changed into a classical NFκB site; second, we previously observed a lack of response to TNF-α of both the oligomerized SNE and the intact SCMV MIE_S reporter genes, compared with stimulation of the HCMV version (11); and third, there was a lack of response to OA by both the isolated SNE motifs as shown here and by the intact SCMV MIEs region as shown previously (11). The latter finding is comparable to the positive effects of OA on the HIV LTR, HCMV MIE, and HCMV IES enhancers and on reconstituted minimal promoters containing oligomerized copies of classical HCMV NFκB motifs. OA is a phosphatase inhibitor that specifically inhibits both PP2A at 50% inhibitory concentrations as low as 1 nM and PP1 at 10 to 15 nM (14). However, two of the four major serine/threonine protein phosphatases, PP2B and PP2C, are unaffected by levels of OA as high as 1 M (14). Addition of OA into a culture medium increases the overall phosphorylation levels of cellular proteins 2.5- to 3-fold, and the functions of several proteins such as elongation factor 2, maturation-promoting factor, p42 mitogen-activated protein kinase (ERK-2), and the AP-1 transcription factor that are controlled by phosphorylation are affected by OA (81). Furthermore, several studies have demonstrated that OA does not inhibit protein tyrosine phosphatase, acid and alkaline phosphatases, inositol triphosphatase, PKA or PKC, and the Ca^{2+}/calmodulin-dependent protein kinases but that it does lead to rapid turnover of IκB and release and transport of active NFκB into the nucleus (76).

Mechanism of SNE or SEE transactivation by synergism. Transcriptional transactivators with homologous amino acid sequences in their DNA binding domains usually constitute a gene family that recognizes similar response or enhancer core motifs. Several families, such as the NFκB/Rel family (5, 80), glucocorticoid receptors, and the ETS (51), CREB, AP-1, and OCT families have been extensively studied. Not only do the members of the same family often interact with each other to form heterodimeric complexes, but members from different families can interact to regulate gene expression synergistically or antagonistically. A directly relevant example comes from studies of serum induction and TPA responses through the SRE motif in the c-Fos promoter (a cellular IE growth response gene). This reaction requires protein-protein contacts between SRF and one or other of two ETS family proteins, SAP-1 or ELK-1 (15, 52, 66, 69).

In CMV, we have found that both basal enhancement and TPA-stimulated activation occurring through the SEE or SNE enhancer motifs, which appear to be present in all primate CMV MIE enhancers, also involve synergistic effects between two essential interacting transcription factors, SRF and ELK-1 (Fig. 11). This arrangement may have evolved to allow differential regulation of the core DNA-binding (SRF) and transactivation (SAP-1 or ELK-1) components. Furthermore, SRF may interact with different ETS family members to allow differential responses to external stimuli such as TPA or serum. Recent studies have found that the ELK-1 and SAP-1 proteins are differentially modified by Ras-dependent and Ras-independent pathways, respectively (7, 29). In addition, several reports have shown that the ETS consensus sequences adjacent to the core SRF sites in the c-Fos SRE are required for TPA-mediated but not for serum-mediated activation (24, 28, 37). The serum-responsive segment of the SRF protein has been mapped to lie within the DNA binding domain. Therefore, perhaps some as yet unidentified cellular factor may be responsible for the serum induction through recognition of a conformational effect on SRF after binding (28). Curiously, we have found that the SCMV SNE motif, unlike the c-Fos SRE, does not respond significantly to serum induction (10, 11). The reason could be either that the spacing between the SRF and ELK-1 binding sites (3 bp instead of 2 bp in the c-Fos SRE) prohibits correctly oriented SRF–SAP-1 complexes from forming or that the different A/T-rich centers of the SNE and SEE core motifs (CCATATATGG) and in the c-Fos SRE (CCATATTAGG) change both the bound SRF conformation and its interaction with the unknown factor (Fig. 10). However, in this arrangement constitutively expressed SRF can still bind to the DNA to prevent chromatin formation and allow rapid access by the inducible transactivators. It is not yet known whether the HCMV SEE motif, which is more similar to the SRE in spacing but more similar to the SNE in the core SRF binding sequence, can act as an SRE (Fig. 10).

The ETS family and cell type specificity. Several ETS family cDNAs, that share properties with TCF, including SAP-1, ELK-1, and NET/SAP-2, have been cloned (15, 30, 60). All three of these ETS subfamily proteins contain homologous amino acid sequences defined as A (ETS DNA binding domain), B (SRF interaction), and C (conserved phosphorylation sites) boxes (84). Activation of the ternary complex requires phosphorylation of the C box of the TCF either through mitogen-activated protein kinase-dependent or -independent pathways. Recent studies have shown that both mitogen-activated protein kinase-dependent and -independent pathways target ELK-1- and SAP-1-related TCFs, respectively (7, 29). In addition, the GGAT ETS DNA binding motif within the c-Fos SRE has now been found to be required for phorbol ester induction but not for serum induction (24, 28, 37). Instead, the A/T-containing central sequence of the core SRE and the DNA binding domain of the SRF appear to be crucial for whole serum induction (28).

Expression of ETS family genes is often tissue specific (4, 67). For example, ETS-1 is expressed at a high level in the thymus but at a low level in the lung and spleen. ELK-1 is expressed predominantly in the lung and testis, and PU1/SPI-1 is expressed primarily in B cells and macrophages. In contrast, ETS-2 is expressed in almost every cell type. Furthermore, there is differential regulation of expression of ETS proteins. Resting T cells express high levels of the ETS-1 but low levels of the ETS-2 RNA and protein, although activated T cells dramatically increase the ETS-2 RNA and protein levels, with

a significant decrease of the ETS-1 RNA and protein levels (4). Since CMV infection is highly tissue specific and shows differential permissiveness in cells at different stages of differentiation, it is very likely that the ELK-1 protein that is involved in interacting with SRF plays an important role in providing tissue-specific IE gene expression. Indeed, our experiments demonstrated that cell-type-specific responses to TPA occur through the SNE sites, because Vero cells (AGM kidney fibroblasts) did not respond to TPA, whereas monocyte lineage U-937 and THP-1 cells, as well as K-562 histiocytic leukemia cells and HL-60 cells, did so strongly. Our EMSA experiments also showed that the SRF–ELK-1 ternary complex could be formed on the SEE motifs with U-937, K-562, HeLa, and HL-60 cell extracts but not with HF, Raji, BALB/c 3T3, or Vero cell extracts. This result probably implies that activation by virion factors in primary lytic infection in HF cells represents an alternative way to induce MIE transcription and that the TPA responses that we are studying here are more likely to be critical for reactivation from a quiescent state in differentiating or activated macrophages and T cells, for example. However, since many other *cis*-acting elements also contribute to the overall basal and inducible MIE enhancer activity, it will be difficult to test the overall significance of the SNE sites in the MIE enhancer background until we are able to find a cell type that depends predominantly on this element for MIE gene regulation.

ACKNOWLEDGMENTS

This study was funded by PHS research grants ROI-A124576 and ROI-AI31454 to G.S.H. from the National Institute of Allergy and Infectious Disease. Y.-J.C. and Q.H. are Ph.D. candidates within the Johns Hopkins Pharmacology Training Program NIH 5T32 MO7626. Y.-J.C. was supported in part by a scholarship from the Ministry of Education, Taiwan, Republic of China.

We thank Pamela Wright for technical assistance and Sarah Heaggans and Wen-Ping Tseng for assistance in preparation of the manuscript.

REFERENCES

1. **Alcendor, D., W. Gu, J.-C. Zong, I. Waheed, R.-S. Peng, Y.-J. Chan, and G. S. Hayward.** Unpublished data.
2. **Alcendor, D. J., P. A. Barry, E. Pratt-Lowe, and P. A. Luciw.** 1993. Analysis of the rhesus cytomegalovirus immediate-early gene promoter. Virology **194:**815–821.
3. **Bellas, R. E., N. Hopkins, and Y. Li.** 1993. The NF-κB binding site is necessary for efficient replication of simian immunodeficiency virus of macaques in primary macrophages but not in T cells in vitro. J. Virol. **67:**2908–2913.
4. **Bhat, N. K., C. B. Thompson, T. Lindsten, C. H. June, S. Fujiwara, S. Koizumi, R. J. Fisher, and T. S. Papas.** 1990. Reciprocal expression of human ETS1 and ETS2 genes during T-cell activation: regulatory role for the protooncogene ETS1. Proc. Natl. Acad. Sci. USA **87:**3723–3727.
5. **Blank, V., P. Kourilsky, and A. Israel.** 1992. NF-kappa B and related proteins: Rel/dorsal homologies meet ankyrin-like repeats. Trends Biochem. Sci. **17:**135–140.
6. **Boshart, M., F. Weber, G. Jahn, K. Dorsch-Hasler, B. Fleckenstein, and W. Schaffner.** 1985. A very strong enhancer is located upstream of an immediate early gene of human cytomegalovirus. Cell **41:**521–530.
7. **Buscher, D., R. A. Hipskind, S. Krautwald, T. Reimann, and M. Baccarini.** 1995. Ras-dependent and -independent pathways target the mitogen-activated protein kinase network in macrophages. Mol. Cell. Biol. **15:**466–475.
8. **Chan, Y. J., and G. S. Hayward.** 1996. Two distinct upstream regulatory domains containing multicopy cellular transcription factor binding sites provide basal repression and inducible enhancer characteristics to the immediate-early IES (US3) promoter from human cytomegalovirus. J. Virol. **70:**5312–5328.
9. **Chang, Y. N., S. Crawford, J. Stall, D. R. Rawlins, K. T. Jeang, and G. S. Hayward.** 1990. The palindromic series I repeats in the simian cytomegalovirus major immediate-early promoter behave as both strong basal enhancers and cyclic AMP response elements. J. Virol. **64:**264–277.
10. **Chang, Y. N., K. T. Jeang, C. J. Chiou, Y. J. Chan, M. Pizzorno, and G. S. Hayward.** 1993. Identification of a large bent DNA domain and binding sites for serum response factor adjacent to the NFI repeat cluster and enhancer region in the major IE94 promoter from simian cytomegalovirus. J. Virol. **67:**516–529.
11. **Chiou, C. J., Y. J. Chan, and G. S. Hayward.** Phorbol ester stimulation induces expression from multiple response elements in the major immediate-early enhancer regions of human and simian cytomegalovirus in monocyte and lymphocyte cell types and can lead to activation of the full lytic cycle in non-permissive U-937 cells. Submitted for publication.
12. **Chiou, C. J., J. Zong, I. Waheed, and G. S. Hayward.** 1993. Identification and mapping of dimerization and DNA-binding domains in the C terminus of the IE2 regulatory protein of human cytomegalovirus. J. Virol. **67:**6201–6214.
13. **Christy, B. A., L. F. Lau, and D. Nathans.** 1988. A gene activated in mouse 3T3 cells by serum growth factors encodes a protein with "zinc finger" sequences. Proc. Natl. Acad. Sci. USA **85:**7857–7861.

13a. **Crawford, S., J. Fallon, and G. S. Hayward.** Unpublished data.

14. **Cohen, P., S. Klumpp, and D. L. Schelling.** 1989. An improved procedure for identifying and quantitating protein phosphatases in mammalian tissues. FEBS Lett. **250:**596–600.
15. **Dalton, S., and R. Treisman.** 1992. Characterization of SAP-1, a protein recruited by serum response factor to the c-fos serum response element. Cell **68:**597–612.
16. **Dignam, J. D., R. M. Lebovitz, and R. G. Roeder.** 1983. Accurate transcription initiation by RNA polymerase II in a soluble extract from isolated mammalian nuclei. Nucleic Acids Res. **11:**1475–1489.
17. **Dutko, F. J., and M. B. Oldstone.** 1981. Cytomegalovirus causes a latent infection in undifferentiated cells and is activated by induction of cell differentiation. J. Exp. Med. **154:**1636–1651.
18. **Fietze, E., S. Prosch, P. Reinke, J. Stein, W.-D. Docke, G. Staffa, S. Loning, S. Devaux, F. Emmrich, R. von Baehr, D. H. Kruger, and H.-D. Volk.** 1994. Cytomegalovirus infection in transplant recipients: the role of tumor necrosis factor. Transplantation **58:**675–680.
19. **Fish, K. N., A. S. Depto, A. V. Moses, W. Britt, and J. A. Nelson.** 1995. Growth kinetics of human cytomegalovirus are altered in monocyte-derived macrophages. J. Virol. **69:**3737–3743.
20. **Forbes, B. A., C. A. Bonville, and N. L. Dock.** 1990. The effects of a promoter of cell differentiation and selected hormones on human cytomegalovirus infection using an in vitro cell system. J. Infect. Dis. **162:**39–45.
21. **Ghazal, P., C. DeMattei, E. Giulietti, S. A. Kliewer, K. Umesono, and R. M. Evans.** 1992. Retinoic acid receptors initiate induction of the cytomegalovirus enhancer in embryonal cells. Proc. Natl. Acad. Sci. USA **89:**7630–7634.
22. **Ghazal, P., H. Lubon, B. Fleckenstein, and L. Hennighausen.** 1987. Binding of transcription factors and creation of a large nucleoprotein complex on the human cytomegalovirus enhancer. Proc. Natl. Acad. Sci. USA **84:**3658–3662.
23. **Gonczol, E., P. W. Andrews, and S. A. Plotkin.** 1984. Cytomegalovirus replicates in differentiated but not in undifferentiated human embryonal carcinoma cells. Science **224:**159–161.
24. **Graham, R., and M. Gilman.** 1991. Distinct protein targets for signals acting at the c-fos serum response element. Science **251:**189–192.
25. **Hermiston, T. W., C. L. Malone, P. R. Witte, and M. F. Stinski.** 1987. Identification and characterization of the human cytomegalovirus immediate-early region 2 gene that stimulates gene expression from an inducible promoter. J. Virol. **61:**3214–3221.
26. **Herrera, R. E., P. E. Shaw, and A. Nordheim.** 1989. Occupation of the c-fos serum response element in vivo by a multi-protein complex is unaltered by growth factor induction. Nature (London) **340:**68–70.
27. **Hilfinger, J. M., N. Clark, M. Smith, K. Robinson, and D. M. Markovitz.** 1993. Differential regulation of the human immunodeficiency virus type 2 enhancer in monocytes at various stages of differentiation. J. Virol. **67:**4448–4453.
28. **Hill, C. S., J. Wynne, and R. Treisman.** 1994. Serum-regulated transcription by serum response factor (SRF): a novel role for the DNA binding domain. EMBO J. **13:**5421–5432.
29. **Hipskind, R. A., D. Buscher, A. Nordheim, and M. Baccarini.** 1994. Ras/MAP kinase-dependent and -independent signaling pathways target distinct ternary complex factors. Genes Dev. **8:**1803–1816.
30. **Hipskind, R. A., V. N. Rao, C. G. Mueller, E. S. Reddy, and A. Nordheim.** 1991. Ets-related protein Elk-1 is homologous to the c-fos regulatory factor p62TCF. Nature (London) **354:**531–534.
31. **Hunninghake, G. W., M. M. Monick, B. Liu, and M. F. Stinski.** 1989. The promoter-regulatory region of the major immediate-early gene of human cytomegalovirus responds to T-lymphocyte stimulation and contains functional cyclic AMP-response elements. J. Virol. **63:**3026–3033.
32. **Ibanez, C. E., R. Schrier, P. Ghazal, C. Wiley, and J. A. Nelson.** 1991. Human cytomegalovirus productively infects primary differentiated macrophages. J. Virol. **65:**6581–6588.
33. **Janknecht, R., R. Zinck, W. H. Ernst, and A. Nordheim.** 1994. Functional dissection of the transcription factor Elk-1. Oncogene **9:**1273–1278.
34. **Jeang, K. T., M. S. Cho, and G. S. Hayward.** 1984. Abundant constitutive expression of the immediate-early 94K protein from cytomegalovirus (Colburn) in a DNA-transfected mouse cell line. Mol. Cell. Biol. **4:**2214–2223.
35. **Jeang, K.-T., and W. Gibson.** 1980. A cycloheximide-enhanced protein in cytomegalovirus-infected cells. Virology **107:**362–374.
36. **Jeang, K. T., D. R. Rawlins, P. J. Rosenfeld, J. H. Shero, T. J. Kelly, and G. S. Hayward.** 1987. Multiple tandemly repeated binding sites for cellular nuclear factor 1 that surround the major immediate-early promoters of simian and

human cytomegalovirus. J. Virol. **61:**1559–1570.
37. **Johansen, F. E., and R. Prywes.** 1994. Two pathways for serum regulation of the c-*fos* serum response element require specific sequence elements and a minimal domain of serum response factor. Mol. Cell. Biol. **14:**5920–5928.
38. **Karim, F. D., L. D. Urness, C. S. Thummel, M. J. Klemsz, S. R. McKercher, A. Celada, C. Van Beveren, R. A. Maki, C. V. Gunther, J. A. Nye, et al.** 1990. The ETS-domain: a new DNA-binding motif that recognizes a purine-rich core DNA sequence. Genes Dev. **4:**1451–1453. (Letter.)
39. **Kondo, K., H. Kaneshima, and E. S. Mocarski.** 1994. Human cytomegalovirus latent infection of granulocyte-macrophage progenitors. Proc. Natl. Acad. Sci. USA **91:**11879–11883.
40. **LaFemina, R., and G. S. Hayward.** 1986. Constitutive and retinoic acid-inducible expression of cytomegalovirus immediate-early genes in human teratocarcinoma cells. J. Virol. **58:**434–440.
41. **LaFemina, R. L., and G. S. Hayward.** 1988. Differences in cell-type-specific blocks to immediate early gene expression and DNA replication of human, simian and murine cytomegalovirus. J. Gen. Virol. **69:**355–374.
42. **LaFemina, R. L., M. C. Pizzorno, J. D. Mosca, and G. S. Hayward.** 1989. Expression of the acidic nuclear immediate-early protein (IE1) of human cytomegalovirus in stable cell lines and its preferential association with metaphase chromosomes. Virology **172:**584–600.
43. **LaMarco, K., C. C. Thompson, B. P. Byers, E. M. Walton, and S. L. McKnight.** 1991. Identification of Ets- and notch-related subunits in GA binding protein. Science **253:**789–792.
44. **LaMarco, K. L., and S. L. McKnight.** 1989. Purification of a set of cellular polypeptides that bind to the purine-rich cis-regulatory element of herpes simplex virus immediate early genes. Genes Dev. **3:**1372–1383.
45. **Lang, D., and T. Stamminger.** 1993. The 86-kilodalton IE-2 protein of human cytomegalovirus is a sequence-specific DNA-binding protein that interacts directly with the negative autoregulatory response element located near the cap site of the IE-1/2 enhancer-promoter. J. Virol. **67:**323–331.
46. **Lathey, J. L., and S. A. Spector.** 1991. Unrestricted replication of human cytomegalovirus in hydrocortisone-treated macrophages. J. Virol. **65:**6371–6375.
47. **Lieberman, P. M., J. M. Hardwick, and S. D. Hayward.** 1989. Responsiveness of the Epstein-Barr virus *Not*I repeat promoter to the Z transactivator is mediated in a cell-type-specific manner by two independent signal regions. J. Virol. **63:**3040–3050.
48. **Lieberman, P. M., J. M. Hardwick, J. Sample, G. S. Hayward, and S. D. Hayward.** 1990. The zta transactivator involved in induction of lytic cycle gene expression in Epstein-Barr virus-infected lymphocytes binds to both AP-1 and ZRE sites in target promoter and enhancer regions. J. Virol. **64:**1143–1155.
49. **Liu, B., and M. F. Stinski.** 1992. Human cytomegalovirus contains a tegument protein that enhances transcription from promoters with upstream ATF and AP-1 *cis*-acting elements. J. Virol. **66:**4434–4444.
50. **Liu, R., J. Baillie, J. G. Sissons, and J. H. Sinclair.** 1994. The transcription factor YY1 binds to negative regulatory elements in the human cytomegalovirus major immediate early enhancer/promoter and mediates repression in non-permissive cells. Nucleic Acids Res. **22:**2453–2459.
51. **Macleod, K., D. Leprince, and D. Stehelin.** 1992. The ets gene family. Trends Biochem. Sci. **17:**251–256. (Review.)
52. **Marais, R., J. Wynne, and R. Treisman.** 1993. The SRF accessory protein Elk-1 contains a growth factor-regulated transcriptional activation domain. Cell **73:**381–393.
53. **Nabel, G., and D. Baltimore.** 1987. An inducible transcription factor activates expression of human immunodeficiency virus in T cells. Nature (London) **326:**711–713.
54. **Nelson, J. A., C. Reynolds-Kohler, and B. A. Smith.** 1987. Negative and positive regulation by a short segment in the 5′-flanking region of the human cytomegalovirus major immediate-early gene. Mol. Cell. Biol. **7:**4125–4129.
55. **Niller, H. H., and L. Hennighausen.** 1990. Phytohemagglutinin-induced activity of cyclic AMP (cAMP) response elements from cytomegalovirus is reduced by cyclosporine and synergistically enhanced by cAMP. J. Virol. **64:**2388–2391.
56. **Norman, C., M. Runswick, R. Pollock, and R. Treisman.** 1988. Isolation and properties of cDNA clones encoding SRF, a transcription factor that binds to the c-fos serum response element. Cell **55:**989–1003.
57. **Pizzorno, M. C., and G. S. Hayward.** 1990. The IE2 gene products of human cytomegalovirus specifically down-regulate expression from the major immediate-early promoter through a target sequence located near the cap site. J. Virol. **64:**6154–6165.
58. **Pizzorno, M. C., M. A. Mullen, Y. N. Chang, and G. S. Hayward.** 1991. The functionally active IE2 immediate-early regulatory protein of human cytomegalovirus is an 80-kilodalton polypeptide that contains two distinct activator domains and a duplicated nuclear localization signal. J. Virol. **65:**3839–3852.
59. **Pizzorno, M. C., P. O'Hare, L. Sha, R. L. LaFemina, and G. S. Hayward.** 1988. *trans*-activation and autoregulation of gene expression by the immediate-early region 2 gene products of human cytomegalovirus. J. Virol. **62:**1167–1179.
60. **Price, M. A., A. E. Rogers, and R. Treisman.** 1995. Comparative analysis of the ternary complex factors Elk-1, SAP-1a and SAP-2 (ERP/NET). EMBO J. **14:**2589–2601.
61. **Rice, G. P., R. D. Schrier, and M. B. Oldstone.** 1984. Cytomegalovirus infects human lymphocytes and monocytes: virus expression is restricted to immediate-early gene products. Proc. Natl. Acad. Sci. USA **81:**6134–6138.
62. **Roberts, M. S., A. Boundy, P. O'Hare, M. C. Pizzorno, D. M. Ciufo, and G. S. Hayward.** 1988. Direct correlation between a negative autoregulatory response element at the cap site of the herpes simplex virus type 1 IE175 (alpha 4) promoter and a specific binding site for the IE175 (ICP4) protein. J. Virol. **62:**4307–4320.
63. **Ryan, W. A., Jr., B. R. Franza, Jr., and M. Z. Gilman.** 1989. Two distinct cellular phosphoproteins bind to the c-fos serum response element. EMBO J. **8:**1785–1792.
64. **Sambucetti, L. C., J. M. Cherrington, G. W. Wilkinson, and E. S. Mocarski.** 1989. NF-kappa B activation of the cytomegalovirus enhancer is mediated by a viral transactivator and by T cell stimulation. EMBO J. **8:**4251–4258.
65. **Schrier, R. D., J. A. Nelson, and M. B. Oldstone.** 1985. Detection of human cytomegalovirus in peripheral blood lymphocytes in a natural infection. Science **230:**1048–1051.
66. **Schroter, H., C. G. Mueller, K. Meese, and A. Nordheim.** 1990. Synergism in ternary complex formation between the dimeric glycoprotein p67SRF, polypeptide p62TCF and the c-fos serum response element. EMBO J. **9:**1123–1130.
67. **Seth, A., R. Ascione, R. J. Fisher, G. J. Mavrothalassitis, N. K. Bhat, and T. S. Papas.** 1992. The ets gene family. Cell Growth Differ. **3:**327–334.
68. **Sharrocks, A. D., F. von Hesler, and P. E. Shaw.** 1993. The identification of elements determining the different DNA binding specificities of the MADS box proteins $p67^{SRF}$ and RSRFC4. Nucleic Acids Res. **21:**215–221.
69. **Shaw, P. E., H. Schroter, and A. Nordheim.** 1989. The ability of a ternary complex to form over the serum response element correlates with serum inducibility of the human c-fos promoter. Cell **56:**563–572.
70. **Shore, P., and A. D. Sharrocks.** 1994. The transcription factors Elk-1 and serum response factor interact by direct protein-protein contacts mediated by a short region of Elk-1. Mol. Cell. Biol. **14:**3283–3291.
71. **Sinclair, J. H., J. Baillie, L. A. Bryant, J. A. Taylor-Wiedeman, and J. G. Sissons.** 1992. Repression of human cytomegalovirus major immediate early gene expression in a monocytic cell line. J. Gen. Virol. **73:**433–435.
72. **Stamminger, T., H. Fickenscher, and B. Fleckenstein.** 1990. Cell type-specific induction of the major immediate early enhancer of human cytomegalovirus by cyclic AMP. J. Gen. Virol. **71:**105–113.
73. **Stein, J., H.-D. Volk, C. Liebenthal, D. H. Kruger, and S. Prosch.** 1993. Tumour necrosis factor alpha stimulates the activity of the human cytomegalovirus major immediate early enhancer/promoter in immature monocyte cells. J. Gen. Virol. **74:**2333–2338.
74. **Stenberg, R. M., J. Fortney, S. W. Barlow, B. P. Magrane, J. A. Nelson, and P. Ghazal.** 1990. Promoter-specific trans activation and repression by human cytomegalovirus immediate-early proteins involves common and unique protein domains. J. Virol. **64:**1556–1565.
75. **Stenberg, R. M., D. R. Thomsen, and M. F. Stinski.** 1984. Structural analysis of the major immediate-early gene of human cytomegalovirus. J. Virol. **49:**190–199.
76. **Sun, S. C., S. B. Maggirwar, and E. Harhaj.** 1995. Activation of NF-kappa B by phosphatase inhibitors involves the phosphorylation of I kappa B alpha at phosphatase 2A-sensitive sites. J. Biol. Chem. **270:**18347–18351.
77. **Sundstrom, C., and K. Nilsson.** 1976. Establishment and characterization of a human histiocytic lymphoma cell line (U-937). Int. J. Cancer **17:**565–577.
78. **Taylor-Wiedeman, J., J. G. Sissons, L. K. Borysiewicz, and J. H. Sinclair.** 1991. Monocytes are a major site of persistence of human cytomegalovirus in peripheral blood mononuclear cells. J. Gen. Virol. **72:**2059–2064.
79. **Taylor-Wiedeman, J., P. Sissons, and J. Sinclair.** 1994. Induction of endogenous human cytomegalovirus gene expression after differentiation of monocytes from healthy carriers. J. Virol. **68:**1597–1604.
80. **Thanos, D., and T. Maniatis.** 1995. NF-kappa B: a lesson in family values. Cell **80:**529–532.
81. **Thevenin, C., S. J. Kim, and J. H. Kehrl.** 1991. Inhibition of protein phosphatases by okadaic acid induces AP1 in human T cells. J. Biol. Chem. **266:**9363–9366.
82. **Thomsen, D. R., R. M. Stenberg, W. F. Goins, and M. F. Stinski.** 1984. Promoter-regulatory region of the major immediate early gene of human cytomegalovirus. Proc. Natl. Acad. Sci. USA **81:**659–663.
83. **Treisman, R.** 1986. Identification of a protein-binding site that mediates transcriptional response of the c-fos gene to serum factors. Cell **46:**567–574.
84. **Treisman, R.** 1994. Ternary complex factors: growth factor regulated transcriptional activators. Curr. Opin. Genet. Dev. **4:**96–101.
85. **Wathen, M. W., and M. F. Stinski.** 1982. Temporal patterns of human cytomegalovirus transcription: mapping the viral RNAs synthesized at immediate early, early, and late times after infection. J. Virol. **41:**462–477.
86. **Weinshenker, B. G., S. Wilton, and G. P. Rice.** 1988. Phorbol ester-induced differentiation permits productive human cytomegalovirus infection in a monocytic cell line. J. Immunol. **140:**1625–1631.